Molecular Biology of the Cell
Vol. 12, 3955–3972, December 2001

The *Schizosaccharomyces pombe spo3*$^+$ Gene Is Required for Assembly of the Forespore Membrane and Genetically Interacts with *psy1*$^+$-encoding Syntaxin-like Protein

Taro Nakamura,*† Michiko Nakamura-Kubo,*† Aiko Hirata,‡ and Chikashi Shimoda*§

*Department of Biology, Graduate School of Science, Osaka City University, Osaka 558-8585, Japan; and ‡Department of Integrated Biosciences, Graduate School of Frontier Science, University of Tokyo, Chiba 277-8562, Japan

Submitted April 16, 2001; Revised August 15, 2001; Accepted September 26, 2001
Monitoring Editor: Hugh R. B. Pelham

Formation of the forespore membrane, which becomes the plasma membrane of spores, is an intriguing step in the sporulation of the fission yeast *Schizosaccharomyces pombe*. Here we report two novel proteins that localize to the forespore membrane. *spo3*$^+$ encodes a potential membrane protein, which was expressed only during sporulation. Green fluorescent protein (GFP) fusion revealed that Spo3 localized to the forespore membrane. The *spo3* disruptant was viable and executed meiotic nuclear divisions as efficiently as the wild type but did not form spores. One of the *spo3* alleles, *spo3-KC51*, was dose-dependently suppressed by *psy1*$^+$, which encodes a protein similar to mammalian syntaxin-1A, a component of the plasma membrane docking/fusion complex. *psy1*$^+$ was essential for vegetative growth, and its transcription was enhanced during sporulation. As expected, Psy1 localized to the plasma membrane during vegetative growth. Interestingly, Psy1 on the plasma membrane disappeared immediately after first meiotic division and relocalized to the forespore membrane as the second division initiated. In the *spo3* null mutant, the forespore membrane was initiated but failed to develop a normal morphology. Electron microscopy revealed that membrane vesicles were accumulated in the cytoplasm of immature *spo3*Δ asci. These results suggest that Spo3 is a key component of the forespore membrane and is essential for its assembly acting in collaboration with the syntaxin-like protein.

INTRODUCTION

Gametogenesis of eukaryotes is a developmental process in which diploid cells undergo meiosis to produce specialized germ cells. The equivalent event in the fission yeast *Schizosaccharomyces pombe* is sporulation. This unique process involves the formation of membrane-bounded haploid gametes (spores) within the cytoplasm of the mother cell (ascus). Four haploid nuclei produced by meiotic nuclear divisions are packaged into membranous compartments. This specialized double unit membrane termed the "forespore membrane" (Yoo *et al.*, 1973) is assembled by fusion of vesicles perhaps derived from the endoplasmic reticulum (ER) and/or the Golgi apparatus (Hirata and Tanaka, 1982; Tanaka and Hirata, 1982). The forespore membrane extends progressively along the dividing nucleus during meiosis II and finally encapsulates each haploid nucleus to form a precursor of spore, termed the "prespore." The prespore then matures into the spore, which is covered by a two-layered wall, an inner cell wall, and an outer spore wall (Yoo *et al.*, 1973; Hirata and Tanaka, 1982; Tanaka and Hirata, 1982). Mature spores are finally liberated from an ascus by ascal wall autolysis to begin a new generation (Yoo *et al.*, 1973).

The internal compartmentalization and meiotic nuclear divisions should proceed in a coordinated manner. A key structure linking these two events is the spindle pole body (SPB), a functional equivalent to the centrosome in animal cells, which acts as a microtubule-organizing center. During meiosis II, SPB undergoes a morphological alteration from a compact single plaque to a multilayered expanded structure (Hirata and Tanaka, 1982; Tanaka and Hirata, 1982; Hagan and Yanagida, 1995). When the SPB modification is blocked by a mutation of the SPB component Spo15, sporulation is

§ Corresponding author. E-mail address: shimoda@sci.osaka-cu.ac.jp.
† The first two authors contributed equally to this work.

totally abolished (Ikemoto *et al.*, 2000). Electron microscopy has revealed that the formation of forespore membranes initiates near the modified SPBs during meiosis II. These observations suggest that SPB plays a crucial role in the spatial and temporal coordination of compartmentalization and nuclear division during gametogenesis.

We have only little information about the origin of small vesicles from which forespore membranes are assembled and the exact mechanism of fusion of these vesicles. Recent studies have indicated that a general protein secretion machinery is implicated in forespore membrane assembly. For example, *S. pombe* Spo20, a Sec14 family phosphatidylinositol-transfer protein, is required for the normal assembly of forespore membranes (Nakase *et al.*, 2001). Another Sec protein Spo14, which is responsible for ER-to-Golgi vesicle transport is also necessary for spore formation in *S. pombe* (Nakamura-Kubo, Nakamura, and Shimoda, unpublished results). Furthermore, several late-acting *SEC* genes (Novick *et al.*, 1981), including *SEC1, SEC4,* and *SEC9,* are required for sporulation in the budding yeast *Saccharomyces cerevisiae* (Neiman, 1998). The membrane fusion machinery, composed of v-SNARE and t-SNARE proteins, governs the specificity of docking and fusion between vesicles and target membranes (Rothman and Orci, 1992; Sollner *et al.*, 1993; Pelham, 1999; McNew *et al.*, 2000). Interestingly, formation of the prospore membrane in budding yeast (equivalent to the forespore membrane in fission yeast) does not require one of the t-SNARE components, Sec9 (an SNAP-25 homolog); instead, its sporulation-specific counterpart, Spo20, is indispensable (Neiman, 1998). These findings imply that precursor vesicles for spore membranes are provided through a general secretory pathway and that sporulation-specific components are substituted in some cases.

Genetic analyses of lots of sporulation-deficient *S. pombe* mutants (Bresch *et al.*, 1968, Kishida and Shimoda, 1986) have identified *spo1*$^+$–*spo20*$^+$ genes. These *spo* gene products may be involved in the individual steps of sporulation; structural alteration of SPBs, supply of precursor vesicles, extension of forespore membranes and their encapsulation of sister nuclei, and synthesis and deposition of spore wall materials. Cytological studies have assigned some of the *spo* gene products to several different steps of sporulation (Ikemoto *et al.*, 2000; Nakamura *et al.*, 2000; Nakase *et al.*, 2001).

In this article, we report the structure and function of the *spo3*$^+$ gene product. Spo3 has a role in spore morphogenesis, because our previous electron microscopic analysis showed that *spo3* mutants form spore-like bodies that resemble spores but contain no nucleus (Hirata and Shimoda, 1992). This EM study prompted us to identify the *spo3*$^+$ gene product and establish its role in spore morphogenesis. We also describe the characterization of the multicopy suppressor of *spo3* mutants. This gene, named *psy1*$^+$, encodes a novel syntaxin 1A-like protein, whose budding yeast and mammalian counterparts act as a specific t-SNARE component for plasma membranes. Indeed, Psy1 localizes to the plasma membrane during vegetative growth. Notably, however, Psy1 translocates to the forespore membrane after second meiotic division. With the use of GFP fused to Spo3 and Psy1 as molecular markers for the forespore membrane, dynamic features of its assembly are monitored focusing on the coordination between this unique membrane assembly process and meiotic nuclear divisions.

MATERIALS AND METHODS

Yeast Strains, Media, and Culture Conditions

S. pombe strains used in this study are listed in Table 1. Sporulation-deficient mutants of *S. pombe*, *spo3-B3* and *spo3*(*spo19*)*-KC51*, were isolated by Bresch *et al.* (1968) and Kishida and Shimoda (1986), respectively. The complete medium YEA supplemented with 75 μg/ml adenine sulfate and 50 μg/ml uracil was used for growth. Malt extract medium MEA and synthetic sporulation media SSA, SSL−N and MM−N were used for mating and sporulation. These media were described by Egel and Egel-Mitani (1974), Gutz *et al.* (1974), and Moreno *et al.* (1990). *S. pombe* cells were grown and sporulated at 28°C. For synchronous meiosis, diploid strains harboring *pat1-114*^{ts} homozygously were cultured in MM−N at 24°C for 18 h, and then the temperature was shifted to 34°C to induce meiosis (Iino *et al.*, 1995). Procedures for transformation of *S. cerevisiae* with plasmid DNA in the presence of lithium acetate have been described (Ito *et al.*, 1983). The *S. cerevisiae* strains used in this study are also listed in Table 1.

Cloning of spo3$^+$

A homothallic *spo3-B3* mutant (MK3L) was transformed with *S. pombe* genomic libraries, pTN-L1 (this study) and a pDB248′-based library (a gift from Dr. Y. Watanabe), containing *Sau*3AI fragments constructed in multicopy plasmids, pAL-KS (Tanaka *et al.*, 2000) and pDB248′ (Beach and Nurse, 1981), respectively. The Leu$^+$ transformants were sporulated on SSA plates and exposed to iodine vapor (Gutz *et al.*, 1974). Those colonies that turned brown were removed as candidates for sporulation-proficient transformants. Plasmids were transferred from such Spo$^+$ and Leu$^+$ transformants to *Escherichia coli* (DH5α). Two plasmids, each from different libraries, were independently isolated and further analyzed. Partial DNA sequencing of the inserts revealed that their sequences were identical to the cosmid clone SPAC607 (EMBL/GenBank/DDBJ accession No.CAB63797.1). The inserts of both plasmids contained an overlapping sequence of ~4 kb (Figure 1A). This region represents one large uninterrupted open reading frame (ORF), SPAC607.10. The cloned gene is shown to be *spo3*$^+$ itself, but not a multicopy suppressor, as described below.

We found that a mutant allele previously known as *spo19-KC51* (Kishida and Shimoda, 1986) was a mutation in the *spo3* locus. First, a *spo3*$^+$-borne plasmid complemented the sporulation defect of the *spo19* mutant (Figure 1B). Second, neither the *spo19-KC51/spo3-B3* nor *spo19-KC51/spo3::ura4*$^+$ diploid strains sporulated. Hereafter, the *spo19-KC51* allele is denoted as *spo3-KC51*.

Plasmid Construction

Plasmids used in this study are listed in Table 2. Plasmid pIL2 was constructed by inserting the 2.2-kb fragment containing the *S. cerevisiae* LEU2 gene into the *Ssp*I site of pBluescript II KS$^-$ (Stratagene, La Jolla, CA). Plasmid pTN218 was constructed by inserting the 1.1-kb *Not*I-*Sac*I fragment, which contains the 3X HA epitope and *nmt1* terminator region of pSLF272 (Forsburg and Sherman, 1997), into pIL2. Plasmids pTN54 and pTN178 were constructed as follows. Two oligonucleotides were used to amplify a mutant version of the *Aequorea* green fluorescence protein gene, *GFP*^{S65T} (a gift from Y. Hiraoka) by PCR with the use of 5′-CCCCTCGAG(*Xho*I)TATGAGTAAAGGAGAA-3′ and 5′-CCCGGATCC(*Bam*HI)GTCGACTTGTATAGTTCATCCATGCCATGTGTAATCCC-3′ as primers. The PCR product was digested with *Xho*I and *Bam*HI and then subcloned into the *Sal*I-*Not*I site of pREP41 and pREP81 (Maundrell, 1993), yielding pTN54 and pTN178, respectively. Plasmid pTN133 was constructed by inserting the 2.3-kb *Pst*I-*Sac*I fragment of pSLF272, which contains the *nmt1* promoter, 3X HA epitope tag, and *nmt1* terminator into the same site of pREP41. pTN197 was constructed by inserting the 1.8-kb *Not*I-*Sac*I fragment of pTN143 (Ikemoto *et al.*, 2000), which contains GFP and the nmt1 terminator

Table 1. Strains

Strain	Genotypes	Source
Schizosaccharomyces pombe		
L968	h^{90}	Leupold
MKW5	h^{90}	This study
B3	h^{90} *spo3-B3 ade6-M210*	Egel *et al.* (1968)
KC51	h^{90} *spo3 (spo19)-KC51 ade6-M210*	Kishida *et al.* (1986)
TN4	h^{-} *leu1-32*	This study
TN8	h^{90} *leu1-32*	This study
TN29	h^{90} *leu1-32 ura4-D18*	Ikemoto *et al.* (2000)
TN47	h^{+s} *ade6-M216*	This study
TN53	h^{-} *ade6-M210*	This study
MK3L	h^{90} *spo3-B3 leu1-32*	This study
MK19L	h^{90} *spo3-KC51 leu1*	This study
MK19U	h^{90} *spo3-KC51 ura4-D18*	This study
MK3004	h^{90} *spo3::ura4*$^{+}$ *ura4-D18*	This study
MKD3	h^{90} *spo3::ura4*$^{+}$ *leu1-32 ura4-D18*	This study
TN180	h^{90} *spo3-GFP≪LEU2 leu1-32*	This study
TN187	h^{90} *spo3-HA≪LEU2 leu1-32*	This study
TN203	h^{+s} *spo3::ura4*$^{+}$ *ade6-M216 ura4-D18*	This study
TN205	h− *spo3::ura4*$^{+}$ *ade6-M210 ura4-D18*	This study
TN56	h^{+s}/h^{-} *ade6-M210/ade6-M216*	This study
TN207	h^{+s}/h^{-} *spo3::ura4*$^{+}$*/spo3::ura4*$^{+}$ *ade6-M210/ade6-M216 ura4-D18/ura4-D18*	This study
JZ670	h^{-}/h^{-} *pat1-114/pat1-114 ade6-M210/ade6-M216 leu1-32/leu1-32*	M Yamamoto
AB4	h^{-}/h^{-} *mei4::ura4*$^{+}$*/mei4::ura4*$^{+}$ *pat1-114/pat1-114 ade6-M210/ade6-M216 leu1-32/leu1-32 ura4-D18/ura4-D18*	Abe and Shimoda (2000)
TN189	h^{-}/h^{-} *pat1-114/pat1-114 ade6-M210/ade6-M216 leu1-32/leu1-32 spo3-HA≪LEU2/spo3*$^{+}$	This study
TN75	h^{90}/h^{90} *ade6-M210/ade6-M216 leu1-32/leu1-32 ura4-D18/ura4-D18*	This study
TN226	h^{90} *spo15-GFP≪LEU2 spo3::ura4*$^{+}$ *leu1-32 ura4-D18*	This study
TN225	h^{90}/h^{90} *psy1::ura4*$^{+}$*/psy1*$^{+}$ *ade6-M210/ade6-M216 leu1-32/leu1-32 ura4-D18/ura4-D18*	This study
Saccharomyces cerevisiae		
H403	*Mata sso1-δ1::URA3 ade2-1 his3-11,15 leu2-3,112 trp1-1 ura3-1*	Aalto *et al.* (1993)
H404	*Matα sso2-δ1::LEU2 ade2-1 his3-11,15 leu2-3,112 trp1-1 ura3-1*	Aalto *et al.* (1993)
TNH405	*Mata/Matα sso1-δ1::URA3 sso2-δ1::LEU2 ade2-1/ade2-1 his3-11,15/his3-11,15 leu2-3,112/leu2-3,112 trp1-1/trp1-1 ura3-1/ura3-1*	This study

region into the same site of pTN133. pAL(spo3-GFP) was constructed as follows. A 6-kb *Bam*HI-*Not*I fragment of pTN(spo3) was inserted into the same site of pTN143, yielding pAL(spo3imGFP). The C terminus of the *spo3*$^{+}$ gene was amplified by PCR with the use of 5′-GCCTTTGTCGCCTCGAGTAATC-3′ and 5′-ATTGCGGCCGC(*Not*I)ACATAATGCGAGGTGG-3′ as primers. The PCR product was digested with *Bgl*II and *Not*I and then ligated into the same sites of pAL(spo3imGFP), yielding pAL(spo3-GFP). pREP41(spo3-GFP) was constructed as follows. Two oligonucleotides 5′-CCCGGATCC(*Bam*HI)AATGGGGATTTTGTCTGTCATCAG-3′ and 5′-ATTGCGGCCGC(*Not*I)ACATAATGCGAGGTGG-3′ were used as primers to amplify the *spo3*$^{+}$ gene by PCR. The PCR product was digested with *Bam*HI and *Not*I and then ligated into the *Bgl*II-*Not*I sites of pTN197, yielding pREP41(spo3-GFP). pREP81(GFP-psy1) was constructed as follows. The *psy1*$^{+}$ gene was amplified by PCR with the use of 5′-CCCGTCGAC(*Sal*I)AATGAATAAAGCAAACG-AT-3′ and 5′-CCCGAGCTC(*Sac*I)ATCTAACCGGCCATATCACT-3′ as primers. The PCR product was digested with *Sal*I and *Sac*I and then ligated into the same sites of pTN178 and pREP41, yielding pREP81(GFP-psy1) and pREP41(psy1), respectively. Plasmid pAL-(spo3 m-GFP) was constructed as follows. The *spo3-KC51* gene by PCR with the use of 5′-CCCGGATCC(*Bam*HI)GACTTATA-ATCTCTTAGATTTCC-3′ and 5′-ATTGCGGCCGC(*Not*I)ACATA-ATGCGAGGTGG-3′ as primers. The PCR product was digested with *Bam*HI and *Not*I and then ligated into the same site of pTN143, yielding pAL(spo3 m-GFP). Plasmid pIL(spo3-HA) was constructed by inserting a 2.8-kb *Sal*I-*Not*I fragment, which contained a 5′-truncated *spo3*$^{+}$ ORF, into pTN218. Plasmid pAL(spo3-HA) was constructed by inserting 1.1-kb *Not*I-*Sac*I fragment of pSLF272, which contains 3X HA epitope tag and *nmt1* terminator into the same sites of pAL(spo3-GFP). Plasmid pREP1(*Not*I) was constructed by inserting the *Not*I linker into the *Sma*I site of pREP1. Plasmid pREP1(SSO1) was constructed as follows. The *SSO1* gene was amplified by PCR with the use of 5′-CCCGGATCC(*Bam*HI)ATGAGT-TATAATAATCCGT-
AC-3′ and 5′-CCCGCGGCCGC(*Not*I)TTAACGCGTTTTGACAAC-3′ as primers. Genomic DNA prepared from *S. cerevisiae* strain W303-1A was used as a template. The PCR product was digested with *Bam*HI and *Not*I and then ligated into the same site of pREP1(*Not*I), yielding pREP1(SSO1). Plasmid pTN284 was constructed as follows. The *Apa*I-*Nhe*I region of pYES2 was eliminated, filled in, and then ligated with *Bgl*II linker, yielding pTN284.5. pTN284.5 was digested with *Bgl*II and ligated with a *Bam*HI fragment bearing the *HIS3* gene, yielding pTN284. Plasmid pTN284(psy1) was constructed as follows. The *psy1*$^{+}$ gene was amplified by PCR with the use of 5′-CCCGGATCC(*Bam*HI)AT-GAATAAAGCAAACGATTATAC-3′ and 5′-CCCGCGGCCGC-(*Not*I)TCAATGTCTATTGCCAAG-3′ as primers. The PCR product was digested with *Bam*HI and *Not*I and then ligated into the same site of pTN284, yielding pTN284(psy1). Plasmid pTN143 (Ikemoto *et al.*, 2000) was digested with *Xba*I-*Stu*I and self-ligated, yielding pTN234. The cohesive end of the fragment was filled-in with KOD polymerase (TOYOBO). pTN234 was then linearized by restricting it

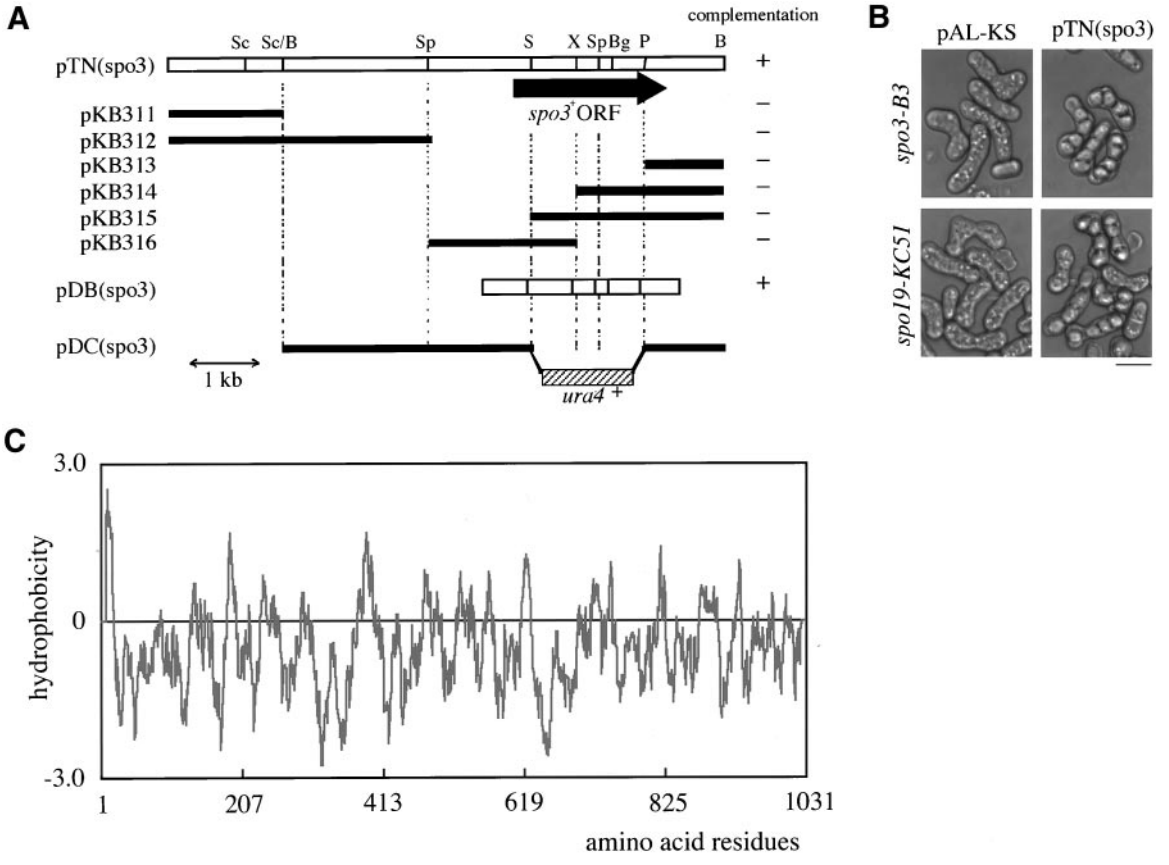

Figure 1. Structure of the *spo3*$^+$ gene. (A) Restriction map, subcloning, and construction of null mutants. The arrow indicates the region and the direction of the *spo3*$^+$ ORF. Subclones pKB311–316 were derived from pTN (spo3). Complementation by each subclone: +, complements; −, does not complement. Restriction enzyme sites: B, *Bam*HI; Bg, *Bgl*II P, *Pst*I; S, *Sal*I; Sc, *Sac*I; Sp, *Sph*I; X, *Xho*I. (B) *spo3*$^+$ suppresses the sporulation defect of *spo19-KC51*. *spo19-KC51* (MK19L) or *spo3-B3* mutant (MK3L) was transformed with either empty (pAL-KS) or *spo3*$^+$-carrying vector (pTN(spo3)). The Leu$^+$ transformants were incubated in sporulation medium (SSA) at 28°C for 2 d. Bar, 10 μm. (C) Hydrophobicity profile of Spo3 obtained according to Kyte and Doolittle (1982). A positive value indicates increasing hydrophobicity.

with *Nsi*I near the center of the sequence and introduced into the TN29 strain.

Gene Disruption

spo3$^+$ was disrupted by replacing a substantial part of the ORF with *ura4*$^+$. An ~8-kb *Bam*HI fragment, which contains the *spo3*$^+$ ORF, was inserted into the same site of pBluescript II-KS$^+$, yielding pBS(spo3). pBS(spo3) was digested with *Kpn*I to eliminate *Sal*I and *Pst*I sites in a multicloning site of the plasmid and self-ligated, yielding pKB279. pKB279 was digested with *Sal*I and *Pst*I, and the 1.7-kb *ura4*$^+$ fragment (Grimm *et al.*, 1988) was inserted into the same sites, yielding pMK286 (Figure 1A). A 5.3-kb *Hin*dIII-*Cla*I fragment containing the disrupted *spo3::ura4*$^+$ allele (*spo3*Δ) was used to transform the strain TN29.

Disruption of *psy1*$^+$ was performed as follows. The *psy1*$^+$ ORF was amplified by PCR with the use of a set of primers, 5′-CCCCTCGAG(*Xho*I)ATCAGGAAAAGTAATTCATC-3′ and 5′-CCCGAGCTC (*Sac*I)ATCTAACCGGCCATATCACT-3′. The 2.4-kb PCR product was digested with *Xho*I and *Sac*I and inserted into the same sites of pBluescript II-KS$^+$, yielding pBS(psy1). pBS (psy1) was digested with *Nru*I and *Nde*I and the 1.7-kb *ura4*$^+$ fragment (Grimm *et al.*, 1988) was inserted into this site, yielding pTN307 (see Figure 7A). A 3.5-kb *Acc*III-*Pst*I fragment containing the disrupted *psy1::ura4*$^+$ allele (*psy1*Δ) was used to transform the strain, TN75. Disruptions were confirmed by genomic Southern hybridization.

Southern and Northern Analysis

Genomic DNA was restricted, fractionated in a 1.0% agarose gel, and then transferred onto nylon membranes (Biodyne B; Pall BioSupport, East Hills, NY). Total RNA was prepared from *S. pombe* cultures (Jensen *et al.*, 1983) and fractionated on a 1.0% gel containing 3.7% formaldehyde according to Thomas (1980).

Western Blotting

The pIL2(spo3)HA plasmid carrying 5′-truncated *spo3* was linearized by restricting it with *Nru*I near the center of the *spo3* sequences and then introduced into the strain TN8. A few Leu$^+$ transformants were tested for sporulation ability. Because these chromosomal integrants (TN187) sporulated, a single copy of spo3-HA proved to be functional. Similarly, the HA-tagged *spo3* was integrated at the *spo3* locus of a diploid strain JZ670. The resulting strain TN189 was used in the following experiments. TN189 was cultured in MM−N at 24°C for 18 h, and the temperature was shifted to 34°C to induce meiosis. At intervals, portions of the culture were sampled, and crude cell extracts were prepared as described by Masai *et al.* (1995).

Table 2. Plasmids used in this study

Plasmid	Characteristics	Source or reference
pAL-KS	*ars1, LEU2*-based vector	Tanaka *et al.* (2000)
pDB248′	*2μ origin, LEU2-based vector*	Beach and Nurse (1981)
pREP1	*ars1, LEU2*-based vector carrying a thiamine-repressible *nmt1* promoter	Maundrell (1993)
pREP41	*ars1, LEU2*-based vector carrying a thiamine-repressible *nmt41* promoter	Maundrell (1993)
pREP81	*ars1, LEU2*-based vector carrying a thiamine-repressible *nmt81* promoter	Maundrell (1993)
pREP42	*ars1, ura4*$^+$-based vector carrying a thiamine-repressible *nmt41* promoter	Maundrell (1993)
pSLF272	3XHA and *nmt1* terminator in pREP42	Forsburg and Sherman (1997)
pTN142	HA and *nmt1* terminator in pAL-KS	This study
pTN143	GFP and *nmt1* terminator in pAL-KS	Ikemoto *et al.* (2000)
pREP1(NotI)	pREP1 having NotI site	This study
pIL2	*LEU2*-based integration vector	This study
pTN54	GFP in pREP41	This study
pTN178	GFP in pREP81	This study
pTN197	GFP in pREP41	This study
pTN133	3XHA and *nmt1* terminator in pREP41	This study
pYES2	*2μ origin, URA3*-based vector carrying a galactose-inducible *GAL1* promoter	Invitrogen
pTN284	*2μ origin, HIS3*-based vector carrying a galactose-inducible *GAL1* promoter	This study
pTN(spo3)	Genomic *spo3*$^+$ isolated from as *S. pombe* genomic library	This study
pDB(spo3)	Genomic *spo3*$^+$ isolated from as *S. pombe* genomic library	This study
pTN(psy1)	*psy1*$^+$ cDNA isolated from as *S. pombe* cDNA library	This study
pTN218	3XHA and *nmt1* terminator in pIL2	This study
pAL(spo3-GFP)	*spo3*$^+$ in pTN143	This study
pAL(spo3-HA)	*spo3*$^+$ in pTN142	This study
pIL2(spo3-HA)	*spo3*$^+$ in pTN218	This study
pREP41(psy1)	*psy1*$^+$ in pREP41	This study
pREP41(spo3-GFP)	*spo3*$^+$ in pTN178	This study
pREP41(GFP-psy1)	*psy1*$^+$ in pTN54	This study
pREP81(GFP-psy1)	*psy1*$^+$ in pTN197	This study
pAL(spo3m-GFP)	*spo3-KC51* in pAL-KS	This study
pBS(spo3)	*spo3*$^+$ in pBluescript II-KS$^+$	This study
pKB279	*spo3*$^+$ in pBluescript II-KS$^+$	This study
pMK286	for *spo3* disruption	This study
pBS(psy1)	*psy1*$^+$ in pBluescript II-KS$^+$	This study
pTN307	for *psy1* disruption	This study
pREP1(SSO1)	*SSO1* in pREP1(*Not*I)	This study
pTN284(psy1)	*psy1*$^+$ in pTN284	This study
pTN234	*LEU2*-based vector carrying a *spo15-GFP*	This study

Polypeptides were separated by SDS-PAGE on a 10% gel and then blotted onto a polyvinylidene difluoride membrane (Millipore, Bedford, MA). Filters were probed with the rat anti-HA antibody 3F10 (Boehringer Mannheim, Mannheim, Germany) at a 1:1000 dilution. Blots were also probed with the anti–α-tubulin antibody, TAT-1 (Woods *et al.*, 1989), to ensure that approximately equal amounts of protein were loaded. Immunoactive bands were revealed by chemiluminescence (NEN Life Sciences, Boston, MA) with horseradish peroxidase-conjugated goat anti-rat IgG (Biosource International, Camarillo, CA) for 3F10 or with goat anti-mouse IgG (Promega, Madison, WT) for TAT-1.

Endoglycosidase H Treatment

TN8 carrying pAL(spo3-HA) was cultured in SSL−N at 28°C for 8 h. The culture (20 ml) was harvested, washed with water, resuspended in 100 μl of 20 mM Tris-HCl (pH 8.0), and heated at 90°C for 5 min. Then 100 μl of 50 mM Tris-HCl (pH 8.0) containing 1 mM PMSF was added to the sample and vortexed with an equal volume of acid-washed glass beads for 3 min. Samples were divided in half, brought to final concentrations of 0.3% SDS, 0.15 M sodium citrate (pH 5.5), and 5 mM NaN_3, and treated with or without 0.05 unit/ml endoglycosidase H (EndoH; Boehringer Mannheim, Mannheim, Germany) at 37°C for 18 h. Spo3-HA proteins were resolved by SDS-PAGE and detected by Western blotting with rat anti-HA antibody (3F10).

Immunofluorescence Microscopy

For cell fixation, we followed the procedure of Hagan and Hyams (1988) with the use of glutaraldehyde and paraformaldehyde. The SPB was visualized by indirect immunofluorescence microscopy with the use of rabbit anti-Sad1 antibody (a gift from O. Niwa; Kazusa DNA Research Institute) and Alexa 546–conjugated goat anti-rabbit IgG (Molecular Probes, Eugene, OR) at a 1:1000 dilution. For microtubule staining, the anti–α-tubulin antibody TAT-1 (Woods *et al.*, 1989) was used with Cy3-conjugated anti-mouse IgG (Amersham Pharmacia Biotech, Uppsala, Sweden) at a 1:1000 dilution. The nuclear chromatin region was stained with DAPI at 1 μg/ml. Stained cells were observed under a fluorescence microscope (model BX50; Olympus, Tokyo, Japan) and Cool SNAP CCD camera (Roper Scientific, San Diego, CA).

Isolation of Multicopy Suppressor of spo3

A homothallic *spo3-KC51* mutant (MK19U) was transformed with an *S. pombe* cDNA library, pTN-RC5 (this study), containing meiotic cDNA fragments constructed in the expression vector pREP42

(Maundrell, 1993). One of 100,000 transformed colonies was able to sporulate. Plasmid DNA (pTN(psy1)) was recovered from *E. coli*. Partial DNA sequencing of the insert revealed that it contained the ORF, SPCC875.03C, which had been identified by the *S. pombe* genome project.

Electron Microscopy

S. pombe cells were fixed with 3% glutaraldehyde in potassium phosphate buffer (pH 7.0). Fixed cells were washed several times in buffer and treated with Zymolyase 60,000 (0.1 mg/ml; Kirin Brewery Co., Takasaki, Japan) in the same buffer at 30°C. The disintegration of the cell wall was examined under a phase-contrast microscope. The Zymolyase-treated cells were washed again in buffer and postfixed in 2% OsO_4 for 2 h at room temperature. After washing in distilled water, they were soaked in a 0.5% aqueous solution of uranyl acetate for 2 h and embedded in agar blocks. The cells were dehydrated by passing them through a series of increasing concentrations of ethanol and absolute acetone, and then they were embedded in Spurr's resin. Sections were stained with uranyl acetate and lead citrate or 0.05% alkali bismuth. Sections were viewed with a JEOL 200CX electron microscope (Peabody, MA) at 100 kV.

RESULTS

spo3⁺ Encodes a Potential Membrane Protein

To elucidate the molecular function of the *spo3⁺* gene product, we isolated *spo3⁺* from an *S. pombe* genomic library by functional complementation (see MATERIALS AND METHODS). Two plasmids, pTN(spo3) and pDB(spo3), could rescue the *spo3-B3* mutant (Figure 1B). Subcloning experiments and partial sequencing revealed that the *spo3*-complementing ability was due to one uninterrupted ORF (SPAC607.10), which is composed of 3084 nucleotides (Figure 1A). This cloned gene was genetically identified as *spo3⁺* as described in the following section. The *spo3⁺* gene has a coding capacity for a 119-kDa protein composed of 1028 amino acids. The deduced amino acid sequence shares no homology with any proteins in the databases. A hydropathic profile and prediction of the secondary structure revealed that Spo3 contains one potential membrane-spanning domain in its amino terminus (Figure 1C). Other functional motifs could not be found.

spo3⁺ Is Not Essential for Growth

To examine whether *spo3⁺* is an essential gene, one-step gene disruption was carried out (Figure 1A). The obtained disruptant harboring the *spo3*Δ allele did not differ from *spo3⁺* in growth rate, cell size, and shape in complete medium, indicating that *spo3⁺* was not essential for normal growth. As expected, this null mutant was asporogenous like the original *spo3-B3* mutant. MKD3 (h^{90} *spo3::ura4⁺*) was crossed to B3 (h^{90} *spo3-B3*). The resulting diploid strain could not sporulate, showing that the cloned gene is allelic to *spo3⁺* but not a multicopy suppressor gene.

Because most of the meiosis-defective mutants isolated to date are not able to initiate sporulation, it is possible that *spo3*Δ has a defect in meiosis. Thus, we studied meiotic nuclear divisions in *spo3*Δ. The kinetics of meiotic division in the diploid strain TN207 harboring *spo3::ura4⁺* homozygously was monitored by nuclear staining with DAPI. First and second meiotic divisions proceeded with kinetics similar to the isogenic wild-type strain TN56 (Figure 2). The final yield of tetranucleate cells reached ~90%. These results suggest that the *spo3*Δ mutant is able to complete meiosis but is defective in ascospore formation.

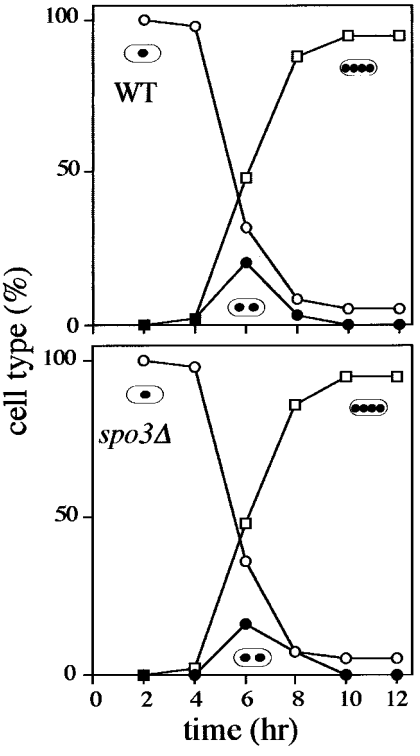

Figure 2. Kinetics of meiosis in the wild type (WT) and a *spo3*Δ mutant. TN207 (*spo3*Δ) and TN56 (wild-type) precultured overnight in liquid growth medium (MM+N) were incubated with shaking at 28°C in liquid sporulation medium (MM−N). A portion of the culture was stained with DAPI. Meiotic cells were classified by the number of nuclei per cell. For each sample, ~500 cells were counted. This figure is based on one representative result of three independent experiments that provided similar results. ○, mononucleate; ●, binucleate; □, tri- or tetranucleate cells.

Transcriptional Regulation of spo3⁺

Like other *S. pombe* genes responsible for sexual reproduction, the *spo3⁺* transcript was not detected in vegetative cells and markedly accumulated during sporulation. Next, the exact timing of *spo3⁺* transcription during synchronous meiosis was determined. Fairly good synchrony in meiotic divisions was attained by inactivation of the temperature-sensitive *pat1–114* allele (see MATERIALS AND METHODS; Iino *et al.*, 1995). Northern blot analysis (Figure 3A) revealed that *spo3* mRNA was barely detectable in vegetative cells at 0 h and abruptly increased at 7 h after induction when cells were in early second meiotic division (Figure 3B).

The *mei4⁺* gene encodes a forkhead transcription factor that regulates many genes required for meiosis and sporulation (Horie *et al.*, 1998; Abe and Shimoda, 2000). To determine whether Mei4 governs *spo3⁺* transcription, we examined the induction of *spo3⁺* in the *mei4*Δ mutant. As shown in Figure 3A, accumulation of the *spo3⁺* mRNA was com-

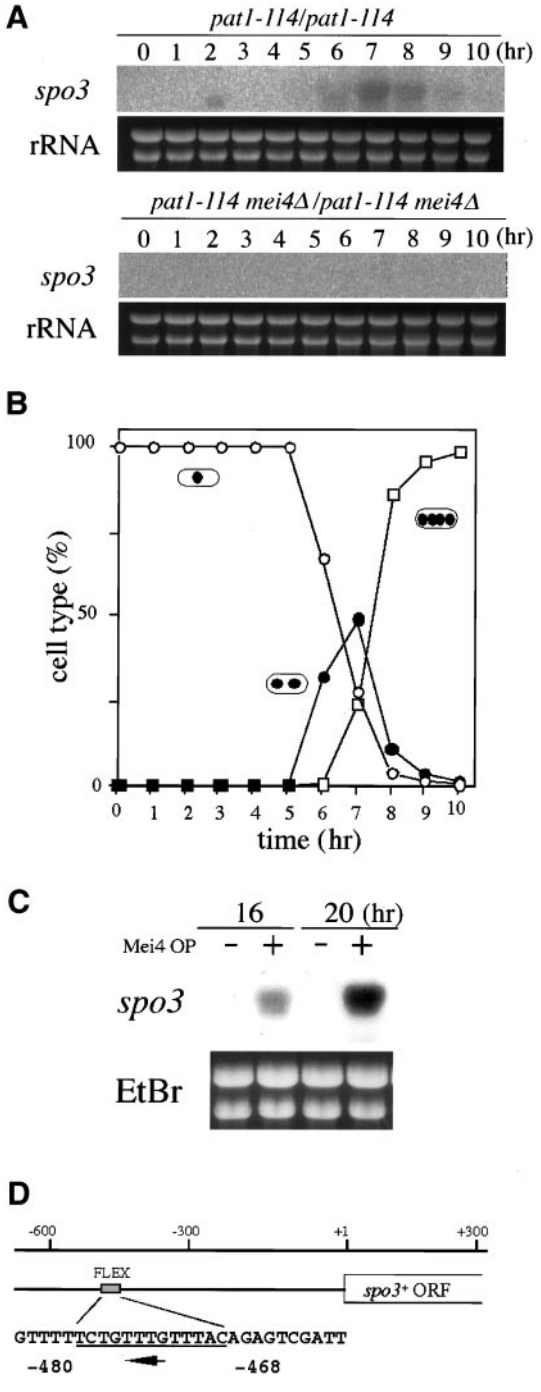

Figure 3. Expression of the *spo3*$^+$ gene during meiosis. (A) The transcription of *spo3*$^+$ in *pat1*-driven synchronous meiosis. Meiosis of the diploid strains harboring homozygous *pat1-114*, JZ670 (*mei4*$^+$), and AB4 (*mei4*Δ), was synchronous. At intervals total RNA was prepared and analyzed by Northern blot hybridization as described in MATERIALS AND METHODS. The approximate quantity of RNA was checked by staining gels with ethidium bromide, which reveals rRNA. (B) Meiotic nuclear division of JZ670 was monitored by DAPI staining. ○, mononucleate; ●, binucleate; □, tri- or tetranucleate cells. (C) The transcription of *spo3*$^+$ is induced by ectopic overproduction of Mei4. TN4 cells harboring plasmid pREP1(*mei4*$^+$) were grown in MM medium (Mei4 OP +) to derepress the *nmt1* promoter. After 16- and 20-h incubation, total RNA was subjected to Northern analysis. (D) The position of the FLEX consensus in the *spo3*$^+$ promoter region. The arrow indicates the direction of FLEX sequence.

pletely abolished in the *mei4*Δ mutant. Furthermore, ectopic overexpression of *mei4*$^+$ induced *spo3*$^+$ mRNA in vegetative cells (Figure 3C). We found that *spo3*$^+$ has a consensus recognition sequence of Mei4, GTAAACAAACAgA (Horie *et al.*, 1998; Abe and Shimoda 2000) in the 5′ upstream region (Figure 3D). We conclude that transcription of *spo3*$^+$ during meiosis is strictly regulated by Mei4.

Changes in the Spo3 Level during Meiosis

The abundance of Spo3 during meiosis was monitored with the use of the chromosomally integrated *spo3-HA* (see MATERIALS AND METHODS). The TN189 strain carrying the *pat1-114* mutation and *spo3-HA* was cultured at 34°C to induce synchronous meiosis. Spo3-HA was not detectable in vegetative cells (at 0 h) and appeared when meiosis II began (5 h) as a 130-kDa band on SDS-PAGE (Figure 4, A and B). This apparent molecular mass was consistent with that deduced from the sequence data. Spo3 became more abundant when cells proceeded to meiosis II (6–7 h). Once meiosis was completed, Spo3-HA was no longer detectable. We conclude that Spo3 is transiently produced in meiotic cells.

Spo3 contained five potential N-glycosylation sites (NxS/T). So we attempted to demonstrate the glycosylation of Spo3 by detecting electrophoretic mobility shift of Spo3-HA by the treatment of endoglycosydase H (EndoH). The TN8 strain transformed with pAL(spo3-HA) was incubated in SSL−N sporulation medium for 8 h. As shown in Figure 4C, the immunoreactive band due to Spo3-HA was very sharp, and the mobility was not affected by EndoH treatment, suggesting that Spo3 was not N-glycosylated.

Spo3-GFP Localizes to the Forespore Membrane

Sequencing of the *spo3*$^+$ gene suggested that its product might have a transmembrane domain in the amino terminus. To verify whether Spo3 resides in cellular membranes, we examined the subcellular localization of Spo3-GFP. A single copy of the *spo3-GFP* fusion gene could complement the sporulation defect of the *spo3*Δ mutant, showing that Spo3-GFP is fully functional. A multicopy plasmid pAL (Spo3-GFP) was introduced into h^{90} *spo3*$^+$ strain TN8. The transformed cells were cultured in sporulation medium (SSL−N). The meiotic stage of the cells was determined by staining their chromatin regions with DAPI and SPBs with anti-Sad1 antibodies. As expected from the Western analysis, Spo3-GFP signal was not detectable in vegetative cells or early in meiosis (see Figure 4). At metaphase II, however, the Spo3-GFP fluorescence became evident near nuclei (Figure 5, A and B). The fluorescent signals presented as a pair of semicircles, their concave sides being opposite to each other. An enlarged view of the metaphase-II nucleus indicates that the Spo3-GFP signal appeared on the cytoplasmic surface of the SPB (Figure 5B). The semicircles then extended in harmony with sister chromatid separation and eventually closed to encapsulate each meiotic nucleus at the end of

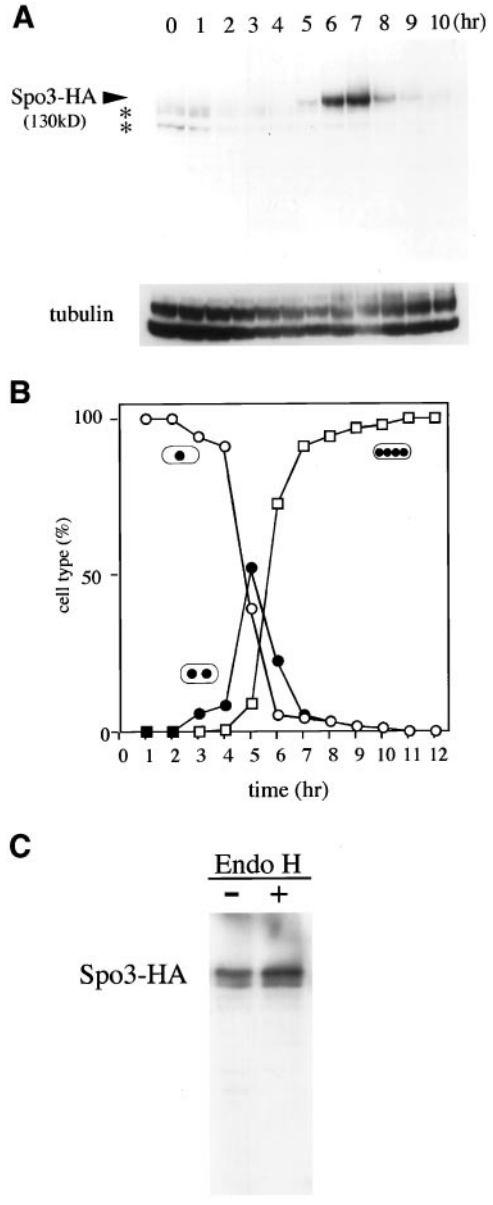

Figure 4. Time course of expression of Spo3 during meiosis. (A) Cells homozygous for *spo3-HA* (TN189) were allowed to proceed through synchronous meiosis. Aliquots were removed at hourly intervals, and protein extracts were subjected to immunoblot analysis with the rat anti-HA antibody 3F10 as well as with anti–α-tubulin antibody as the loading control. Asterisks indicate nonspecific bands. (B) Meiotic nuclear division was monitored by counting the number of nuclei per cell. ○, mononucleate; ●, binucleate; □, tri- or tetranucleate cells. (C) Mobility of Spo3-HA treated with endoglycosidase H.

meiosis II (Figure 5A). Essentially identical data were obtained with strains harboring a single copy of the spo3-GFP fusion allele integrated chromosomally. Previous electron microscopic observations have shown that the forespore membrane initiates near outer plaques of the meiosis-II SPB and then elongates along the nuclear membrane (Hirata and Tanaka, 1982). The observed development of the fluorescent image strongly suggested that Spo3-GFP localized to the forespore membrane. The signal of Spo3-GFP disappeared when mature spores were discernible by phase-contrast microscopy (Figure 5C). This observation is consistent with the Western data in Figure 4, which shows that Spo3 disappeared at a postmeiotic stage.

An inner leaflet of the forespore membrane is presumed to become the plasma membrane in spores, implying that both types of membrane are closely related. We thus next tested whether Spo3-GFP localized to the plasma membrane, when expressed ectopically by the *nmt1* promoter in vegetative cells. Figure 5E shows that Spo3-GFP is preferentially present at the cell surface and in septa, suggesting its localization to the plasma membrane.

The *spo3-KC51* mutant exhibited a strict sporulation-deficient phenotype like *spo3* disruptants. We next determined the mutation point of the *spo3-KC51* allele. The *spo3-KC51* mutant gene was obtained by PCR (see MATERIALS AND METHODS) and sequenced. *spo3-KC51* harbored an opal nonsense codon at the 427th tryptophan residue (Figure 5E). Thus this allele might produce a truncated protein, referred to as Spo3m, missing the C-terminal two-thirds of the full-length product. To test whether Spo3m is adequately localized to the forespore membrane, Spo3m-GFP was expressed in wild-type cells. As shown in Figure 5F, this truncated protein was found in the forespore membrane, suggesting that the N-terminal 426 amino acids of Spo3 are enough for the proper localization and that sporulation defect of *spo3-KC51* was not due to the mislocalization of the protein product.

Overexpression of Syntaxin 1A-like Protein Rescued spo3 Mutation

To gain insight into the role of *spo3*$^+$ in forespore membrane formation, we isolated a multicopy suppressor that complements the sporulation deficiency of *spo3*. A homothallic haploid strain MK19U harboring *spo3-KC51* was transformed with an *S. pombe* cDNA library constructed in the expression vector, pREP42 (Maundrell, 1993). Approximately 100,000 transformants were screened for their sporulation ability by the iodine vapor method. We isolated one iodine-positive sporogenic transformant and recovered a plasmid pTN(psy1), which carried the *psy1*$^+$ gene (see below). Spores formed by pTN(psy1) were apparently immature (Figure 6A), and the number of asci was less than those formed by pAL(spo3) (Figure 6B). pTN(psy1) complemented *spo3-B3* and *spo3::ura4*$^+$ only slightly (Figure 6, A and B). These results indicate that the *psy1*$^+$ cDNA clone rescued the *spo3-KC51* mutation only partially in an allele-specific and dose-dependent manner.

Partial sequencing identified this multicopy suppressor as SPCC825.03C (EMBL/GENBANK/DDBJ Accession No. AL122011) encoding a mammalian syntaxin 1A-like protein. This gene was thus designated as *psy1*$^+$ after *S. pombe* syntaxin-like protein. The *psy1*$^+$ gene encodes a 32.5-kDa protein composed of 285 amino acid residues (Figure 7B). The putative *psy1*$^+$ gene product shares 34 and 28% identity and 65 and 54% similarity with the budding yeast syntaxin homologue, Sso1 (Aalto *et al.*, 1993), and human syntaxin-1A (Bennett *et al.*, 1992), respectively. Psy1 contains a potential transmembrane domain composed of 23 amino acid resi-

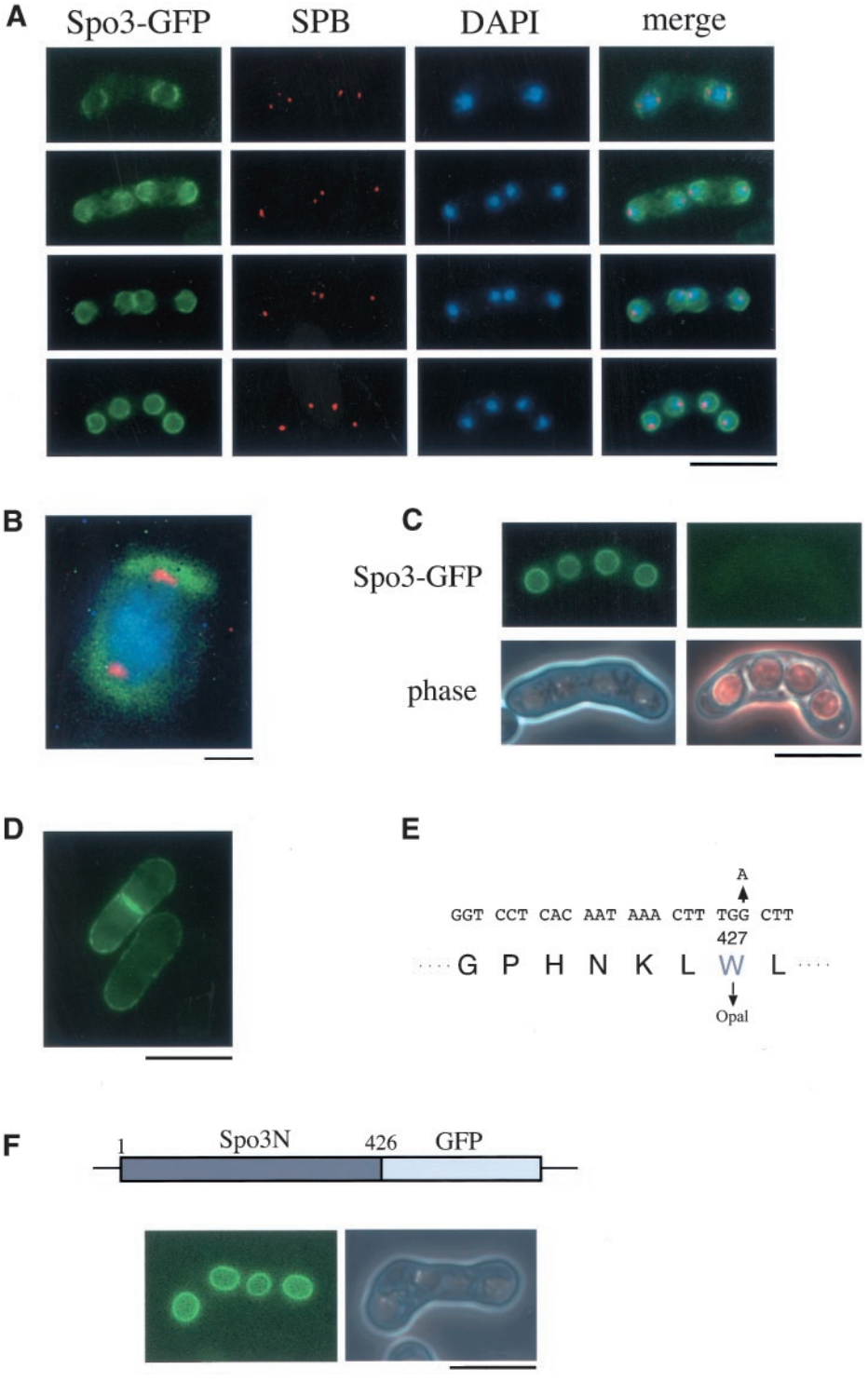

Figure 5. Localization of Spo3 during meiosis and sporulation. (A) A homothallic haploid strain TN8 (h^{90} *spo3*$^{+}$) carrying pAL(spo3-GFP) was cultured in SSL−N to induce meiosis. Cells fixed at different stages of meiosis were stained with DAPI. SPBs were visualized by anti-Sad1 antibody and GFP fluorescence was observed under a fluorescence microscope. Bar, 10 μm. (B) Magnified and merged image of a metaphase-II nucleus. Blue, DAPI; orange, SPB; green, Spo3-GFP. Bar, 1 μm. (C) Spo3-GFP signal was not observed in mature spores. Bar, 10 μm. (D) Ectopic expression of Spo3-GFP in vegetative cells. TN8 cells carrying pREP41 (spo3-GFP) were cultured in SSL+N at 25°C for 12 h. Bar, 10 μm. (E) The *spo3-KC51* mutant allele carries a single nucleotide change (from G to A) which results in an opal nonsense codon at tryptophan 427. (F) The protein product of *spo3-KC51*, Spo3 m, localizes to the forespore membrane. TN8 cells carrying pAL(spo3 m-GFP) were grown on SSA plates at 25°C for 1 d.

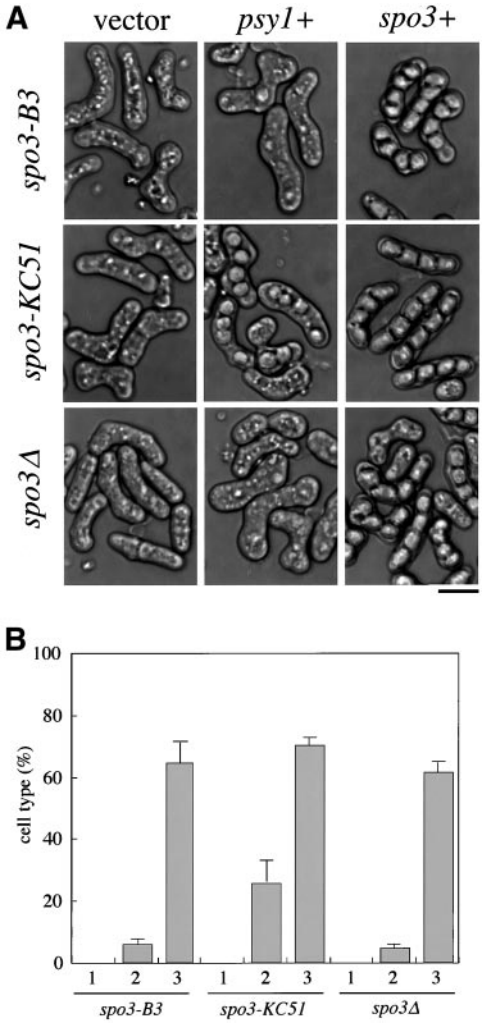

Figure 6. Isolation of *psy1*$^+$ as a multicopy suppressor of *spo3-KC51*. (A) MK19L (h^{90} *spo3-KC51*), MK3L (h^{90} *spo3-B3*) and MKD3 (h^{90} *spo3::ura4*$^+$) were transformed with a multicopy plasmid carrying either *psy1*$^+$ or *spo3*$^+$. The transformants were cultured on sporulation medium (SSA) at 28°C for 3 d. (B) Sporulation efficiency of the transformants. Three independent transformants were examined for percent asci. Mean values with SEs are presented. Plasmids used are (1) pREP41, (2) pREP41(psy1), or (3) pAL(spo3).

dues in the carboxyl terminal region and two α-helical coiled-coil domains (Figure 7C). The C-terminal coiled-coil domain is known as a syntaxin motif, which is required for four-helix bundles formed from syntaxin, SNAP-25, and synaptobrevin family proteins (Gotte and von Mollard, 1998). These structural features strongly suggest that Psy1 functions as a plasma membrane t-SNARE component.

Psy1 Is Essential for Vegetative Growth

S. cerevisiae has two duplicated genes, *SSO1* and *SSO2*, coding for syntaxin-1A homologues (Aalto *et al.*, 1993). Although any single disruptant of *SSO1* and *SSO2* is viable, double disruption results in lethality. By contrast, there is no syntaxin-like protein-encoding gene other than *psy1*$^+$ in the *S. pombe* genome database. *psy1*$^+$ thus seems an essential gene. To verify this, *psy1*$^+$ was disrupted by replacement of a substantial part of the coding region with the *ura4*$^+$ cassette (Figure 7A). After transformation of the *S. pombe* diploid strain TN75 with a linear DNA fragment containing the disrupted allele, *psy1:: ura4*$^+$, Ura$^+$ transformants were obtained. Tetrad analysis of these candidates indicated that most asci produced two viable and two inviable spores, and all viable spores were Ura$^-$ (Figure 7D). Microscopic observation of the inviable progeny showed that these spores germinated but ceased growth after several divisions. Therefore, *psy1*$^+$ is essential for vegetative cell growth and viability.

Next we address the question of whether *S. cerevisiae SSO1* and *S. pombe psy1*$^+$ are functionally equivalent. A plasmid pREP(SSO1) carrying the *SSO1* gene, which could be expressed under the thiamine-repressible *nmt1* promoter, was introduced into an *S. pombe* diploid strain TN225 harboring the *psy1:: ura4*$^+$ allele heterozygously. Diploid transformants were sporulated, and the tetrads were dissected. We found that no *psy1*Δ segregants formed colonies under either induced or repressed conditions, indicating that *SSO1* did not rescue the lethality of *psy1*Δ cells. Reciprocally, *psy1*$^+$ was expressed in *S. cerevisiae*. An expression plasmid pTN284(psy1), in which *psy1*$^+$ was placed under control of the *GAL1* promoter, was introduced into an *S. cerevisiae* diploid strain TNH405 harboring *sso1* and *sso2* heterozygously. The transformants were sporulated and the spore clones were scored. No *sso1 sso2* double mutant was found among progeny colonies, even when cultured on galactose medium. Thus we could not provide evidence that *S. pombe* Psy1 and *S. cerevisiae* Sso1 were functionally equivalent.

Expression of psy1 mRNA

We next examined the transcription of *psy1*$^+$ during meiosis and sporulation. Log-phase cells of a homothallic haploid strain (MKW5) were incubated in the sporulation medium MM−N, and the *psy1*$^+$ mRNA abundance was monitored by Northern analysis (Figure 8A). The mRNA was detected in vegetative cells (0 h sample) and further increased during meiosis. To know exactly the timing of the *psy1*$^+$ mRNA elevation, a similar Northern analysis was carried out with *pat1-114* mutants. The level of *psy1*$^+$ mRNA began to increase at around 3 h and peaked at ~7 h after induction (Figure 8B). We noted that the mRNA level of both *psy1*$^+$ and *spo3*$^+$ peaked about 7 h early in meiosis II (cf. Figure 3, A and C). As stated earlier (Figure 3A), transcription of *spo3*$^+$ was dependent on Mei4. We also observed that the level of *psy1*$^+$ transcript was remarkably reduced in the *mei4*Δ strain (Figure 8B). However, overexpression of *mei4*$^+$ in vegetative cells did not enhance transcription of *psy1*$^+$ (Figure 8C). It appears that *psy1*$^+$ expression is independent of Mei4. In support of this, the promoter region of *psy1*$^+$ has no canonical FLEX-like motif. Repression of *psy1*$^+$ transcription may be an indirect consequence of the meiotic arrest at prophase I in *mei4*Δ. Nevertheless, the prominent increase in *psy1*$^+$ mRNA during meiosis strongly suggests a role of *psy1*$^+$ for meiosis and sporulation.

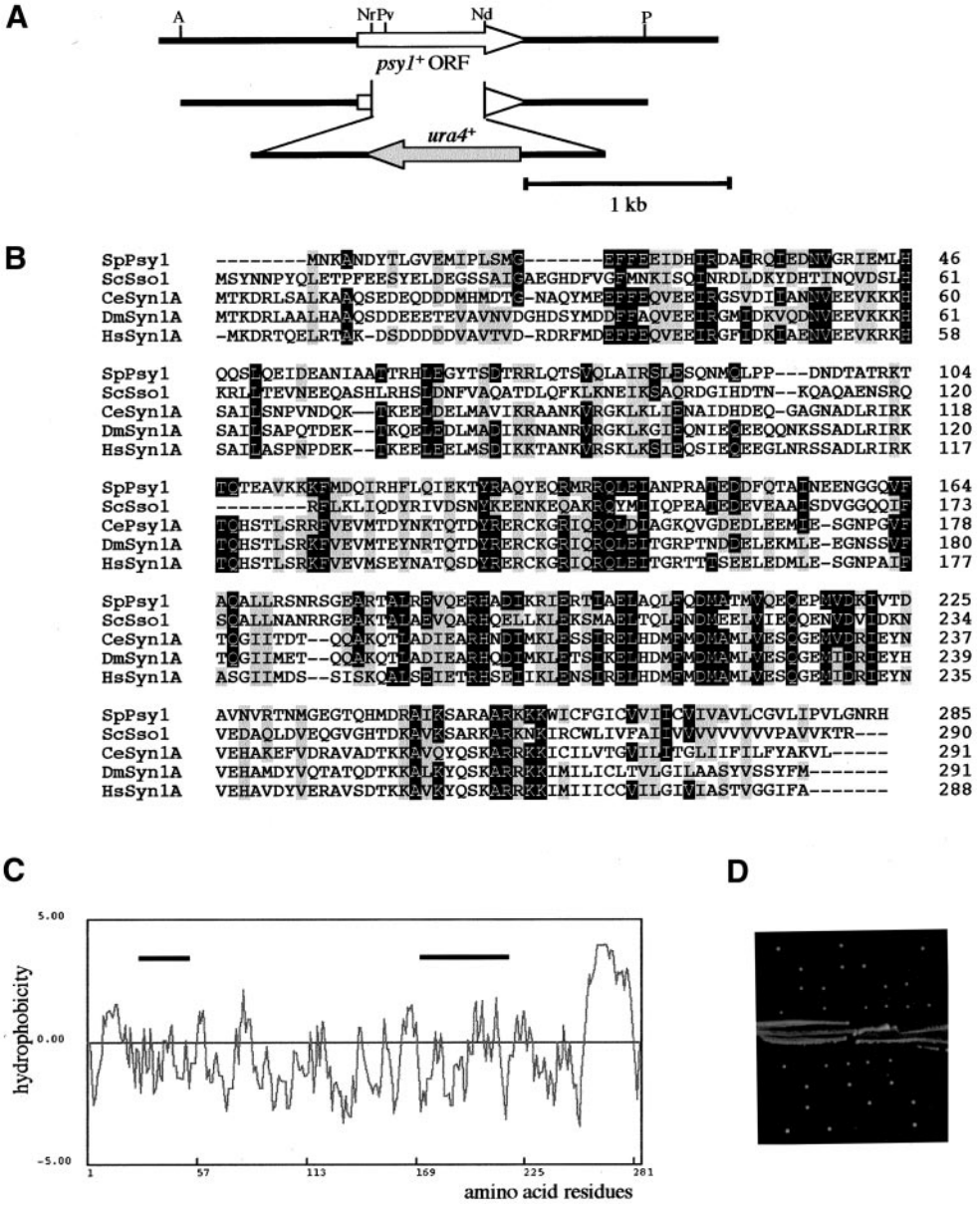

Figure 7. Structure of the *psy1*$^+$ gene and its disruption. (A) A restriction map of *psy1*$^+$. The white arrow indicates the direction and region of the *psy1*$^+$ ORF. The *Acc*III-*Pst*I fragment was used for the disruption. Restriction enzymes sites: A, *Acc*III; Nd, *Nde*I; Nr, *Nru*I; P, *Pst*I; Pv, *Pvu*II. (B) Comparison of the amino acid sequence of Psy1 with the syntaxin-1A homologues from *S. cerevisiae* (ScSso1; Aalto *et al.*, 1993), *Caenorhabditis elegans* (CeSyn1A), *Drosophila melanogaster* (DmSyn1A; Schulze *et al.*, 1995) and *Homo sapiens* (HsSyn1A; Zhang *et al.*, 1995). Identical amino acids are shown in white against black and similar ones are shaded. (C) Hydrophobicity profile of Psy1 according to Kyte and Doolittle (1982). A positive value indicates increasing hydrophobicity. A coiled-coil region was predicted with the use of the COILS program with the 28-residue window setting (Lupas *et al.*, 1991). The putative coiled-coil regions ($p > 0.9$) are shown by bold bars. (D) Viability of *psy1::ura4*$^+$ spores. A diploid (TN225) heterozygous at the *psy1*$^+$ locus (*psy1*$^+$/*psy1::ura4*$^+$) was sporulated and the dissected tetrads were incubated on YEA plates at 25°C for 5 d.

Psy1 Localizes to the Plasma Membrane during Vegetative Growth and to the Forespore Membrane during Sporulation

If Psy1 is an *S. pombe* homolog of syntaxin-1A, it must be present in the plasma membrane. To test this possibility, we constructed the *GFP- psy1*$^+$ fusion gene in which GFP was tagged at the amino terminus of Psy1. The fusion gene was placed downstream of the *nmt1* promoter on a multicopy plasmid pREP81. This plasmid, termed pREP81(GFP-psy1), was harmless to *S. pombe* cells and complemented the lethality of *psy1* null mutants. When the fusion gene was expressed in growing cells, the GFP-Psy1 fluorescence was preferentially found at the cell surface and in the septa (Figure 9A), strongly suggesting the localization of Psy1 to the plasma membrane.

Next, we studied the localization of GFP-Psy1 in meiotic and sporulating cells. Before entering metaphase II, GFP-Psy1 localized to the plasma membrane as in vegetative cells. Surprisingly, the fluorescence on the plasma membrane disappeared when cells proceeded to meiosis II and then appeared as semicircle structures encircling dividing nuclei (Figure 9B). The meiosis-II SPBs were situated at the center of each semicircle (Figure 9C). The GFP-Psy1 structure extended to engulf each of the daughter nuclei that completed meiosis. This behavior of GFP-Psy1 resembles that of Spo3. Thus we conclude that Psy1 is present in the plasma membrane before the second meiotic division and

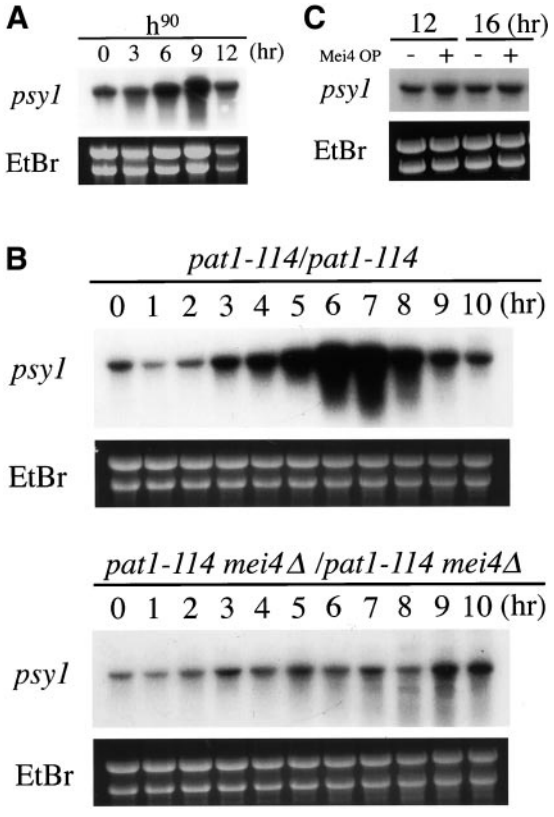

Figure 8. Expression of the *psy1*$^+$ gene during meiosis. (A) Transcription of the *psy1*$^+$ gene. MKW5 (h^{90} wild-type) cells were precultured overnight in MM+N medium and then transferred to MM−N sporulation medium. Total RNA was analyzed by Northern blot hybridization. (B) Transcription of the *psy1*$^+$ gene in *pat1*-driven meiosis. The RNA samples were prepared from JZ670 (*mei4*$^+$) and AB4 (*mei4*Δ). The preparations obtained in the experiment shown in Figure 3 were used. (C) Effect of ectopic expression of *mei4*$^+$ on *psy1*$^+$ transcription. TN8 (h^{90} *leu1-32*) transformed with either pREP1 or pREP1(*mei4*$^+$) was incubated in MM+N at 28°C for 12 and 16 h. The approximate quantity of RNA was checked by staining gels with ethidium bromide.

then relocalizes to the forespore membrane. The GFP-Psy1 signal persisted even after maturation of spores, unlike Spo3, which disappeared in postmeiotic cells (Figure 9D).

Spo3 Function Is Required for Forespore Membrane Assembly

spo3 mutants produce no mature spores, whereas they undergo meiosis with normal kinetics (Figure 2). We next studied defects in spore morphogenesis in more detail. The modification of SPB during meiosis II from a compact plaque to a multilayered structure is a prerequisite to sporulation (Hirata and Shimoda, 1992; Ikemoto *et al.*, 2000). As Spo3 is present in forespore membranes from the early stage of assembly, we suspected that the modification of SPB was impaired by the *spo3* mutation. However, immunofluorescence analysis with the use of the antibody against an SPB component Sad1 showed that modified crescent-shaped SPBs were observed at a frequency comparable to the wild type during second meiotic division (Figure 10A). This conclusion was corroborated by fluorescence microscopic observation of GFP-tagged Spo15, which is another SPB-associated protein (Ikemoto *et al.*, 2000). The fluorescent image also revealed that SPB was modified in meiotic culture of *spo3*Δ (Figure 10B). Therefore, the sporulation defect of the *spo3* mutant is not due to the failure to modify the SPB structure during meiosis II.

Next, we investigated the assembly of forespore membranes in *spo3*Δ with the use of GFP-Psy1. As stated above, the *spo3-KC51* mutation was partially suppressed by overexpression of *psy1*$^+$ under a *nmt1* promoter. However, *psy1*$^+$ under a much weaker promoter in pREP81 did not affect the sporulation-defective phenotype of *spo3*Δ. Therefore, moderately expressed GFP-tagged Psy1 can be adopted as a forespore membrane marker. The *spo3*Δ strain MKD3 was transformed by pREP81(GFP-psy1) and incubated in sporulation medium. Development of the forespore membrane was observed by GFP fluorescence microscopy, and the progression of meiosis was monitored by SPB duplication and elongation of spindle microtubules. In *spo3*Δ cells, the forespore membrane initiated normally near SPBs (Figure 10, C and D), but later development was aberrant (Figure 10E). In most wild-type cells (>90%), the forespore membrane encapsulated each haploid nucleus (Figure 9B). About 70% of the *spo3*Δ zygotes formed four aggregates of GFP-Psy1 near nuclei (Figure 10E upper; class I in Figure 10F). These aberrant structures may represent remnants of collapsed membranes. The rest (~30%) of the *spo3*Δ zygotes contained four nucleated prespores, although they were remarkably small (Figure 10E, bottom; class II in Figure 10F). Sad1 signal for SPBs was very faint in these aberrant cells, although the reason for this is unknown at present. These findings confirm our previous electron microscopic studies showing aberrant prespores in *spo3* mutants (Hirata and Shimoda, 1992). These results indicate that forespore membrane formation initiates normally, but the subsequent development and the integrity of the forespore membrane are impaired in *spo3*Δ.

Because the *spo3-KC51* mutation was suppressed by overexpression of Psy1, fusion of vesicles with the forespore membrane might be defective in *spo3*Δ cells. Fine structures of *spo3*Δ cells incubated in sporulation medium were observed by electron microscopy. As shown in Figure 11, membrane vesicles were remarkable in the cytoplasm of immature *spo3*Δ asci, but such vesicle accumulation was not observed in wild-type asci (Figure 11, A and C). Anucleated spore-like bodies were discernible in *spo3*Δ, as reported previously (Hirata and Shimoda, 1994). The present EM study strongly suggested that Spo3 was implicated in a vesicle fusion process during forespore membrane assembly.

DISCUSSION

Sporulation Is Characterized by Plasma Membrane Formation within the Cytoplasm

Sporulation in yeast is a unique process in that new cells (spores) are constructed inside of the cytoplasm of mother cells (asci). Spores are first delimited by the forespore membrane. The inner leaflet of the forespore membrane becomes the plasma membrane of spores. Development of the fore-

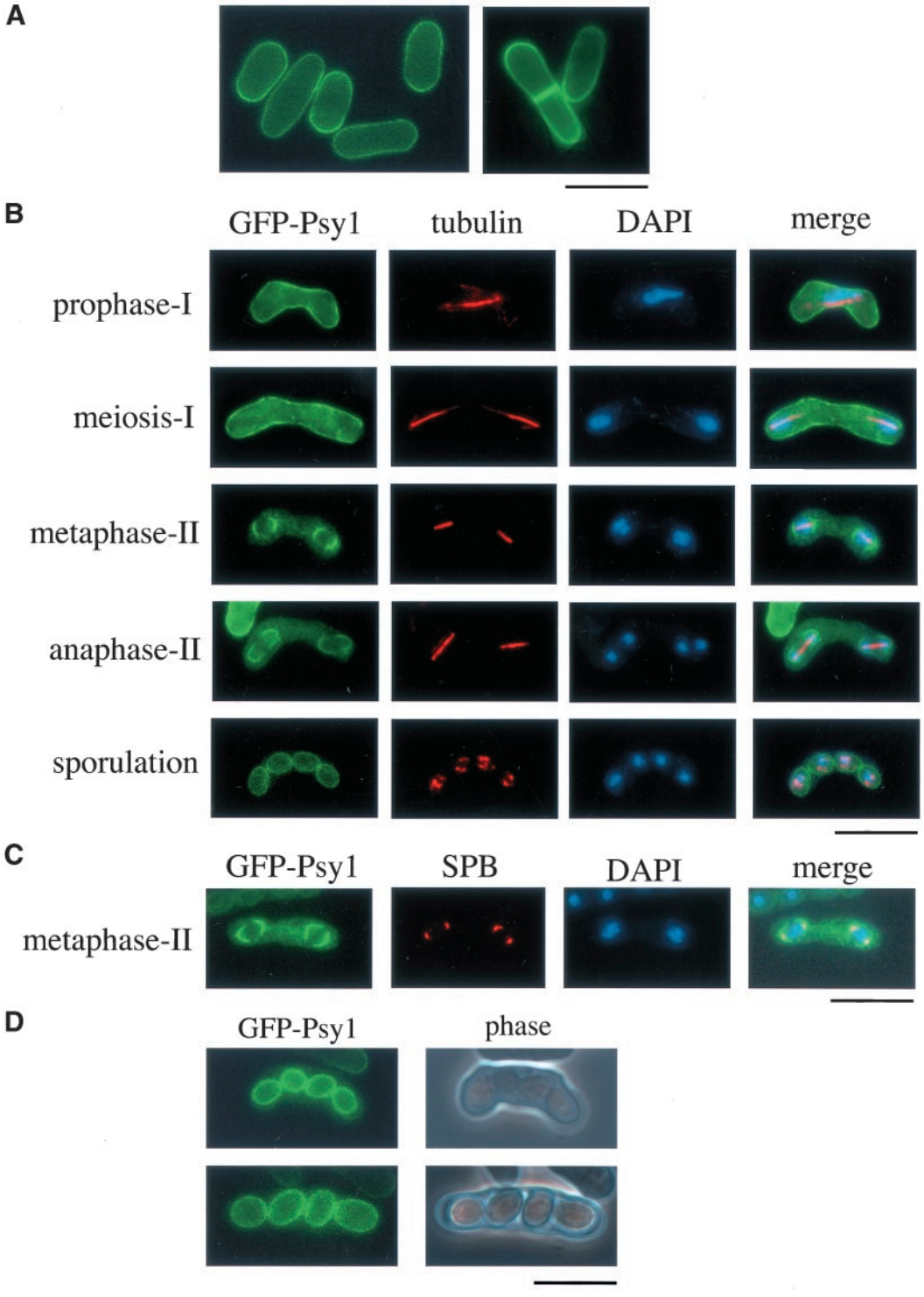

Figure 9. Localization of Psy1. (A) GFP-Psy1 localizes to plasma membrane in vegetative cells. Homothallic haploid strain TN8 carrying pREP81(GFP-psy1) was cultured in SSL+N at 28°C for 12 h. (B and C) Localization of GFP-Psy1 during meiosis and sporulation. The same strain as shown in A was cultured in SSL−N to induce meiosis. Fixed cells at different stages of meiosis were examined by DAPI and GFP, as well as with anti-α-tubulin antibody TAT-1(B) or with anti-Sad1 antibody (C). (D) GFP-Psy1 signal persists in mature spores. TN8 carrying pREP81(GFP-psy1) was sporulated in SSL−N. Mature and immature asci were observed. Bars, 10 μm.

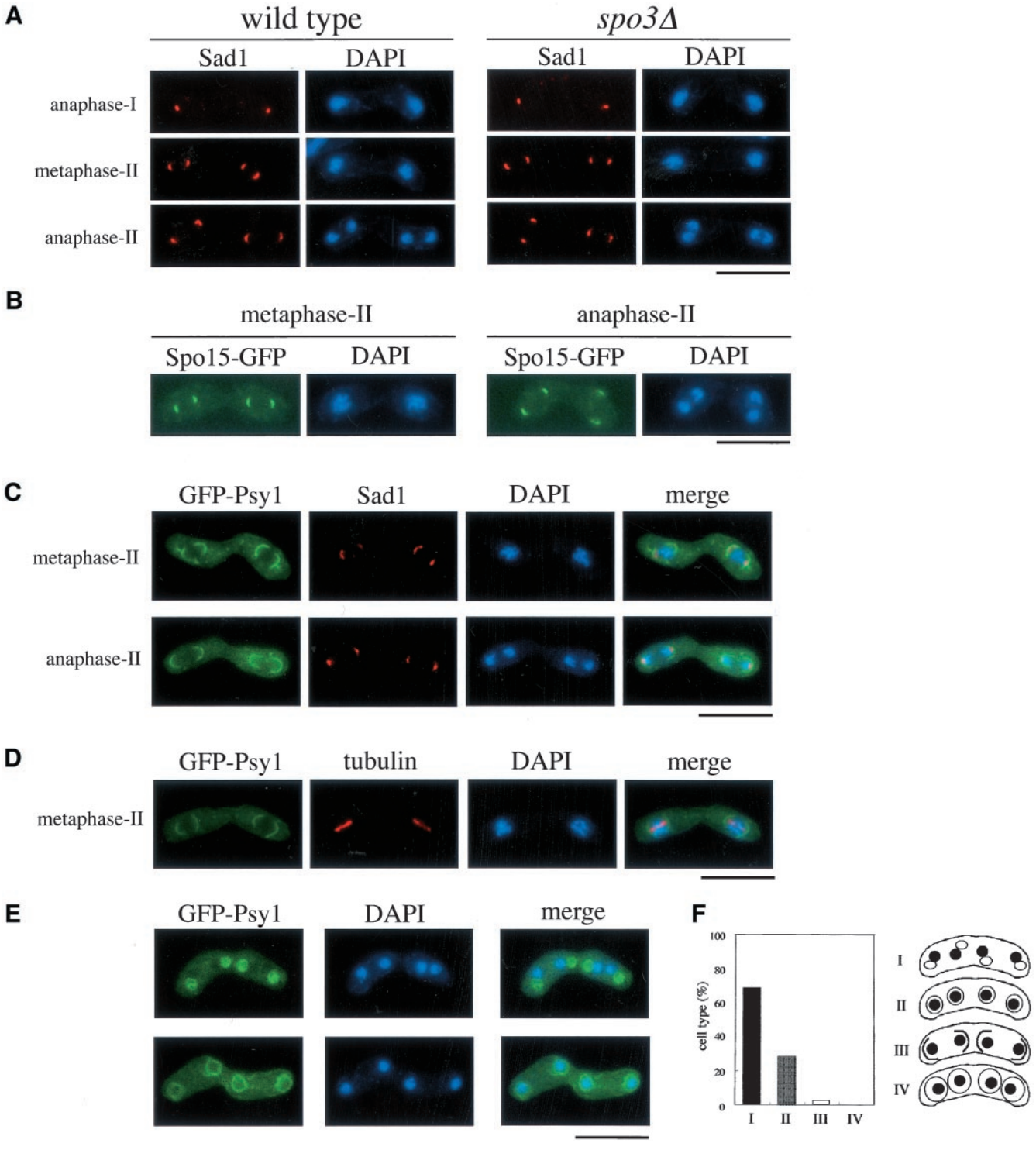

Figure 10. Abnormal sporulation in *spo3*Δ mutant. (A) The morphological change in SPBs from dot to crescent forms during meiosis II is normal in *spo3*Δ. A wild-type strain (MKW5) and a *spo3*Δ mutant strain (MK3004) were cultured in SSL−N sporulation medium and doubly stained with the anti-Sad1 antibody and DAPI. (B) SPB modification in *spo3*Δ as revealed by Spo15-GFP. *spo3*Δ mutant strain harboring Spo15-GFP (TN226) was cultured in SSL−N, fixed, and stained with DAPI. (C and D) *spo3* mutant cells initiate forespore membrane formation normally. MKD3 (h^{90} *spo3*Δ) cells carrying pREP81(GFP-Psy1) were cultured in SSL−N to induce meiosis. Fixed cells were examined with the use of DAPI and GFP, as well as with anti-Sad1 antibody (C) or with anti–α-tubulin antibody TAT-1(D). (E and F) Assembly of forespore membranes and formation of prespores in *spo3*Δ cells. Cells of *spo3*Δ strain (MKD3) transformed with pREP81(GFP-

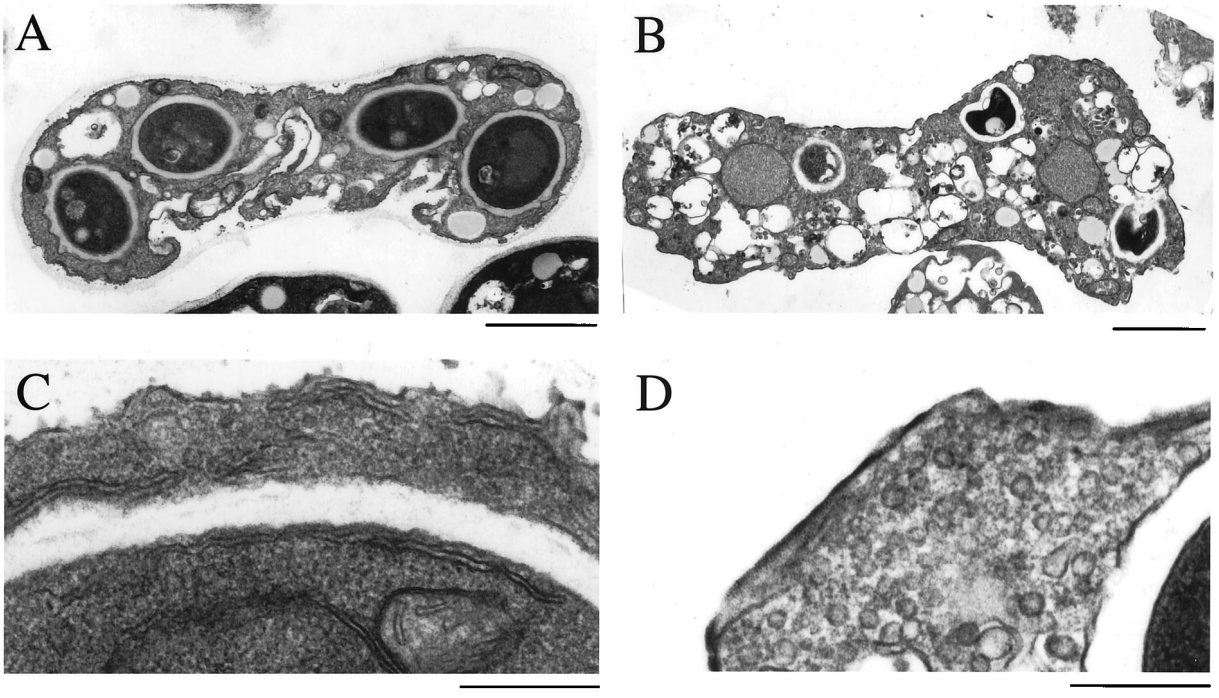

Figure 11. Fine structures of wild-type and *spo3-B3* asci. Mature spores in wild-type (A) and anucleated spore-like bodies in *spo3* mutant (B) are seen. Note that many membranous vesicles are present in the cytoplasm of *spo3*Δ (D). Electron-transparent zones in (C) and (D) are spore walls. Wild-type (A and C), *spo3-KC51* mutant (B and D). Scale bar: A and B, 0.2 μm; C and D, 1 μm.

spore membrane is coordinated with meiotic nuclear divisions in a spatially and temporally controlled manner.

Neiman (1998) pointed out the analogy of forespore membrane formation to membrane assembly in pollen development and cellularization of syncytial blastoderm in *Drosophila* embryogenesis (McCormick, 1993; Loncar and Singer, 1995; Sisson *et al.*, 2000). If a common molecular mechanism for de novo membrane synthesis in the cytoplasm is shared by both yeast and higher eukaryotes, fission yeast sporulation should provide an excellent experimental system.

Little is known about the forespore membrane formation because of the lack of suitable molecular markers. In this article, we report two fission yeast proteins, Spo3 and Psy1, which localize to the forespore membrane, and demonstrate that their GFP-tagged versions are useful to trace the process of forespore membrane assembly.

spo3$^+$ *Encodes a Novel Protein That Localizes to the Forespore Membrane*

The predicted Spo3 protein has no significant sequence similarity to known proteins. Spo3 accumulates during meiosis and abruptly disappears from asci. No degradation signals such as a destruction box or a PEST sequence were found. Spo3 has a hydrophobic potential membrane-spanning domain in its NH_2 terminus (Figure 1C). Indeed, localization of Spo3 to the forespore membrane is not affected by the COOH-terminal truncation (Δaa 427-1028; Figure 5F). The membrane-spanning structure, however, was not predicted with high probability, because two arginine residues were present in this stretch. Therefore, we attempted to demonstrate that Spo3 was actually membrane-integrated protein by subcellular fractionation. Cell-free homogenates were obtained from sporulating cells expressing HA-tagged Spo3 and fractionated by differential centrifugation. However, Western blotting failed to reveal the immunoreactive band due to HA-Spo3 in any fractions. Spo3 seemed extremely unstable protein, because it could be immunologically recognized only under denatured conditions. Overproduction of Spo3-HA driven by the *nmt* promoter did not improve the result.

The forespore membrane is composed of double unit membranes with a lumenal space between them. Given that Spo3 is integrated into the membrane with its extreme N-terminus, the major body of the polypeptide is situated either outside of the membrane or inside of the lumen. The detectable change in apparent molecular weight was not observed after the treatment of Spo3 with endoglycosydase H (Figure 4C), although Spo3 has five potential N-glycosylation sites. This result implies that Spo3 is not N-glycosylated, and perhaps a major part of this possible membrane protein is situated outside of the ER membrane. This topological feature might be maintained on the forespore mem-

Figure 10 (cont). psy1) were cultured in sporulation medium SSL−N. Forespore membranes and chromatin regions were visualized by GFP and DAPI, respectively (E). Bars, 10 μm. (F) Relative frequency of the cell types. Stained cells were categorized into the following 3 classes: class I, four aggregates of GFP-Psy1 were formed close to nuclei (E, top); class II, four prespores were formed but were remarkably small (E, bottom); class III, forespore membranes were formed at the normal site but did not extend; and class IV, four normal prespores were formed.

brane. The Syntaxin family protein spans the membrane by C-terminal domain, exposing the N-terminal region to cytoplasm. We speculate that Spo3 and Psy1 interact each other in the cytoplasmic face of the forespore membrane to facilitate the fusion of vesicles with the forespore membrane.

Visualization of the forespore membrane by GFP-Psy1 revealed that *spo3* mutants were defective in forespore membrane assembly. A majority of the *spo3*Δ zygotes contained four amorphous masses of GFP-Psy1 outside of the nucleus, and the rest contained four very small nucleated prespores (Figure 10E). Thus, *spo3*Δ cells have defects in the assembly process of forespore membranes. We conclude that Spo3 is a forespore membrane component that is required for normal development of prespores.

Electron microscopic studies suggest that the forespore membrane grows by fusion with membrane vesicles, probably derived from the ER or Golgi apparatus. Spo20 is an *S. pombe* homolog of budding yeast Sec14 that is involved in post-Golgi membrane trafficking. In fact, Spo20 is necessary for normal development of the forespore membrane (Nakase *et al.*, 2001). Perhaps Spo3 is involved in fusion of vesicles with the forespore membrane. Less efficient fusion of vesicles to the target membrane may result in small-sized prespores or sometimes in a catastrophic consequence, the collapse of the membrane. This presumptive role of Spo3 might be supported by the fact that the *spo3-KC51* allele is suppressed by an extra copy of *psy1*$^+$ encoding an *S. pombe* plasma membrane t-SNARE. In budding yeast, overexpression of syntaxin homologues, Sso1 and Sso2, enhanced protein secretion and suppressed some late acting *sec* mutants (Ruohonen *et al.*, 1997). Overproduction of Psy1 could enhance the efficiency of vesicle fusion to the target membrane, the forespore membrane in this case. Furthermore, our present EM study revealed that small membrane vesicles were remarkably accumulated in *spo3*Δ immature asci (Figure 11). This observation supports the idea that Spo3 is required for efficient vesicle fusion to the target membrane. Additionally, Spo3 may contribute to the integrity of the forespore membrane architecture. If the function of Spo3 is impaired, the membrane integrity is lost, and subsequently spore-like bodies with abnormal forespore membranes are formed. It is plausible that Spo3 may mediate biogenesis of the spore plasma membrane by maintaining the physicochemical nature of forespore membranes.

Recently, Knop and Strasser (2000) found a prospore membrane protein Don1 in *S. cerevisiae*. There is no similarity in primary structure between Spo3 and Don1. In addition, a genome database search indicates that *S. pombe* has no Don1-like protein. In contrast to Spo3, which localizes throughout the forespore membrane, Don1 is detected only at the leading edge of prospore membranes. Unlike the *spo3*$^+$ gene, the *don1* disruption causes no apparent phenotypes. We suppose that Spo3 and Don1 play different function in assembly of the future plasma membrane of spores.

Role of Psy1 during Sporulation

We identified a novel gene *psy1*$^+$ that encodes a syntaxin-like protein as a multicopy suppressor of *spo3-KC51*. It is supposed that Psy1 is required for not only growth but also sporulation, because *psy1*$^+$ expression is greatly stimulated during meiosis (Figure 8B). Psy1 has a high degree of homology with *S. cerevisiae* Sso1 and Sso2 and mammalian syntaxin-1A (Figure 7B). In addition to the overall sequence similarity, Psy1 contains a hydrophobic putative transmembrane domain and an α-helical coiled-coil region designated as the syntaxin motif in the C-terminal region. Syntaxin is integrated into the plasma membrane by its C-terminal domain and forms a complex with SNAP-25 through the syntaxin motif.

A striking feature of Psy1 is its localization. Psy1 preferentially localizes to the plasma membrane in vegetative cells and changes its localization to the internal membrane compartment during sporulation. At metaphase II, the GFP-Psy1 signal on the plasma membrane disappears and relocalizes to the forespore membrane. There are two possibilities to explain this phenomenon. First, Psy1 on the plasma membrane is degraded at metaphase II, and de novo synthesized Psy1 is exclusively transported to forespore membranes through an ordinary ER/Golgi pathway. Alternatively, the plasma membrane Psy1 is internalized by endocytosis and transported to the forespore membrane. In both hypothetical schema, a spatial and temporal control of Psy1 localization to forespore membrane remains to be analyzed in detail. It was reported that syntaxin1 is required for cellularization of *Drosophila* embryos (Burgess *et al.*, 1997). Neiman *et al.* (2000) recently reported that budding yeast syntaxin homologues, Sso proteins, also relocalized to the prospore membrane. Thus, the plasma membrane syntaxin may also be required for the spore membrane formation in both fission and budding yeasts. The localization mechanism of t-SNARE proteins to the target membrane is still unclear. In this regard, our finding that the *S. pombe* syntaxin homolog translocates during sporulation appears to be important.

Budding yeast has duplicated genes, *SNC1* and *SNC2*, encoding v-SNARE on post-Golgi vesicles (Protopopov *et al.*, 1993). For SNAP-25, this yeast has also two genes, *SEC9* and *SPO20*. Interestingly, Sec9 is active primarily in vegetative cells (Brennwald *et al.*, 1994), whereas Spo20 plays a vital role in the formation of prospore membranes (Neiman, 1998). In contrast, the *S. pombe* genome contains a single unique gene (SPAC6G9.11 and SPBC26H8.02c), each coding for v-SNARE and SNAP-25, respectively. These components of the SNARE complex of fission yeast have not been characterized.

Molecular Mechanisms of Spo3 and Psy1 in the Formation of Forespore Membrane

On the basis of the results of the present study and our previous reports (Ikemoto *et al.*, 2000; Nakase *et al.*, 2001), we propose a model for the construction of the forespore membrane (Figure 12). From metaphase II to anaphase II, the SPB undergoes morphological alteration to a multilayered form, depending on the function of Spo15 (Ikemoto *et al.*, 2000). Two new proteins were also identified as the meiotic SPB component in *S. cerevisiae* (Knop and Strasser, 2000; Bajgier *et al.*, 2001). Membrane vesicles are gathered and fuse to each other on the cytoplasmic face of the modified SPB. Syntaxin-like protein (Psy1) and probably SNAP-25 homolog are recruited to this membrane organization site. These t-SNARE components and the putative v-SNARE protein are involved in the docking and fusion between the putative forespore membrane primordium and post-Golgi vesicles. As anaphase II proceeds, the forespore membrane extends and eventually encapsulates each of the haploid nuclei. Spo3

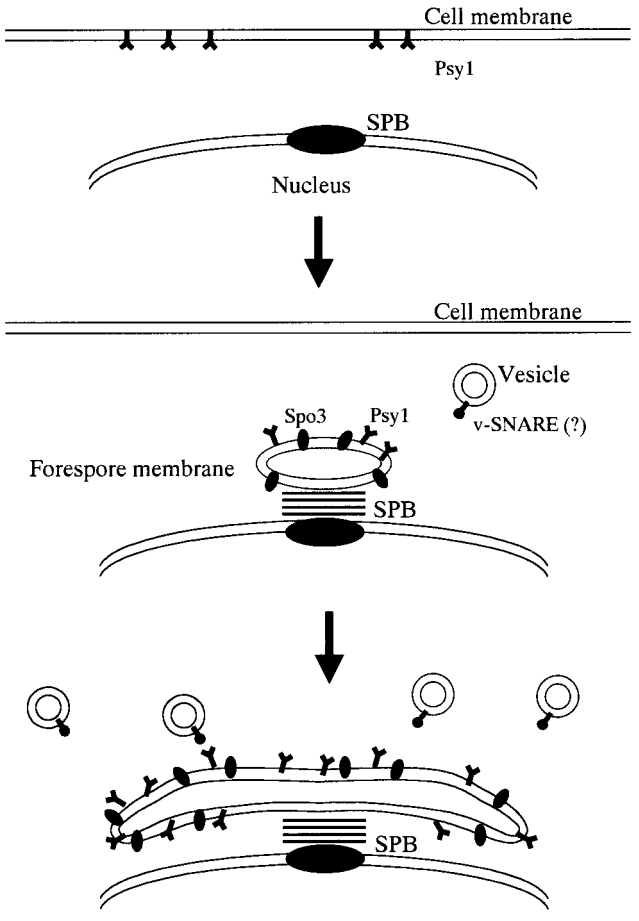

Figure 12. A model for assembly of the forespore membrane.

contributes to the forespore membrane assembly by promoting efficient membrane fusion or stabilizing the nascent forespore membrane architecture. The resulting prespores then mature to ascospores by constructing spore walls. Further molecular analysis of Spo3, Psy1, and other related proteins is necessary to fully understand this intriguing cell assembly process.

ACKNOWLEDGMENTS

We thank A. Nakano and coworkers of RIKEN and K. Takegawa of Kagawa University for invaluable discussions, K. Tanaka of the University of Tokyo, S. Forsburg of the Salk Institute, and Y. Hiraoka of Kansai Advanced Research Center for plasmids, and S. Keranen of VTT Biotechnology Laboratory for yeast strains, K. Gull of the University of Manchester for anti–α-tubulin antibody TAT-1, and O. Niwa of Kazusa DNA Research Institute for affinity-purified antibodies against Sad1. We also thank M. Yamamoto and Y. Watanabe of the University of Tokyo for *S. pombe* genomic library, plasmids, and strains. The present study was partly supported by Grants-in-Aid for Scientific Research on Priority Areas from the Ministry of Education, Science, Sports and Culture of Japan to C.S. and T.N. and Saneyoshi Scholarship Foundation to T.N.

REFERENCES

Aalto, M.K., Ronne, H., and Keranen, S. (1993). Yeast syntaxins Sso1p and Sso2p belong to a family of related membrane proteins that function in vesicular transport. EMBO J. *12*, 4095–4104.

Abe, H., and Shimoda, C. (2000). Autoregulated expression of *Schizosaccharomyces pombe* meiosis-specific transcription factor Mei4 and a genome-wide search for its target genes. Genetics *154*, 1497–1508.

Bajgier, B.K., Malzone, M., Nickas, M., and Neiman, A.M. (2001). Spo21 is required for meiosis-specific modification of the spindle pole body in yeast. Mol. Biol. Cell *12*, 1611–1621.

Beach, D., and Nurse, P. (1981). High efficiency transformation of the fission yeast *Schizosaccharomyces pombe.* Nature *292*, 140–142.

Bennett, M.K., Calakos, N., and Scheller, R.H. (1992). Syntaxin: a synaptic protein implicated in docking of synaptic vesicles at presynaptic active zones. Science *257*, 255–259.

Brennwald, P., Kearns, B., Champion, K., Keranen, S., Bankaitis, V., and Novick, P. (1994). Sec9 is a SNAP-25-like component of a yeast SNARE complex that may be the effector of Sec4 function in exocytosis. Cell *79*, 245–258.

Bresch, C., Muller, G., and Egel, R. (1968). Genes involved in meiosis and sporulation of a yeast. Mol. Gen. Genet. *102*, 301–306.

Burgess, R.W., Deitcher, D.L., and Schwarz, T.L. (1997). The synaptic protein syntaxin1 is required for cellularization of *Drosophila* embryos. J. Cell Biol. *138*, 861–875.

Egel, R., and Egel-Mitani, M. (1974). Premeiotic DNA synthesis in fission yeast. Exp. Cell Res. *88*, 127–134.

Forsburg, S.L., and Sherman, D.A. (1997). General purpose tagging vectors for fission yeast. Gene *191*, 191–195.

Gotte, M., and von Mollard, G.F. (1998). A new beat for the SNARE drum. Trends Cell Biol. *8*, 215–218.

Grimm, C., Kohli, J., Murray, J., and Maundrell, K. (1988). Genetic engineering of *Schizosaccharomyces pombe*: a system for gene disruption and replacement using the ura4 gene as a selectable marker. Mol. Gen. Genet. *215*, 81–86.

Gutz, H., Heslot, H., Leupold, U., and Loprieno, N. (1974). *Schizosaccharomyces pombe*. Handb. Genet. *1*, 395–446.

Hagan, I., and Yanagida, M. (1995). The product of the spindle formation gene *sad1*$^+$ associates with the fission yeast spindle pole body and is essential for viability. J. Cell Biol. *129*, 1033–1047.

Hagan, I.M., and Hyams, J.S. (1988). The use of cell division cycle mutants to investigate the control of microtubule distribution in the fission yeast *Schizosaccharomyces pombe*. J. Cell Sci. *89*, 343–357.

Hirata, A., and Shimoda, C. (1992). Electron microscopic examination of sporulation-deficient mutants of the fission yeast *Schizosaccharomyces pombe*. Arch. Microbiol. *158*, 249–255.

Hirata, A., and Shimoda, C. (1994). Structural modification of spindle pole bodies during meiosis II is essential for the normal formation of ascospores in *Schizosaccharomyces pombe*: ultrastructural analysis of *spo* mutants. Yeast *10*, 173–183.

Hirata, A., and Tanaka, K. (1982). Nuclear behavior during conjugation and meiosis in the fission yeast *Schizosaccharomyces pombe*. J. Gen. Appl. Microbiol. *28*, 263–274.

Horie, S., Watanabe, Y., Tanaka, K., Nishiwaki, S., Fujioka, H., Abe, H., Yamamoto, M., and Shimoda, C. (1998). The *Schizosaccharomyces pombe mei4*$^+$ gene encodes a meiosis-specific transcription factor containing a forkhead DNA-binding domain. Mol. Cell. Biol. *18*, 2118–2129.

Iino, Y., Hiramine, Y., and Yamamoto, M. (1995). The role of *cdc2* and other genes in meiosis in S*chizosaccharomyces pombe.* Genetics *140*, 1235–1245.

Ikemoto, S., Nakamura, T., Kubo, M., and Shimoda, C. (2000). *S. pombe* sporulation-specific coiled-coil protein Spo15p is localized to the spindle pole body and essential for its modification. J. Cell Sci. *113*, 545–554.

Ito, H., Fukuda, Y., Murata, K., and Kimura, A. (1983). Transformation of intact yeast cells treated with alkali cations. J. Bacteriol. *153*, 163–168.

Jensen, R., Sprague, G.F., Jr., and Herskowitz, I. (1983). Regulation of yeast mating-type interconversion: feedback control of HO gene expression by the mating-type locus. Proc. Natl. Acad. Sci. USA *80*, 3035–3039.

Kishida, M., and Shimoda, C. (1986). Genetic mapping of eleven spo genes essential for ascospore formation in the fission yeast *Schizosaccharomyces pombe*. Curr. Genet. *10*, 443–447.

Knop, M., and Strasser, K. (2000). Role of the spindle pole body of yeast in mediating assembly of the prospore membrane during meiosis. EMBO J. *19*, 3657–3667.

Kyte, J., and Doolittle, R.F. (1982). A simple method for displaying the hydropathic character of a protein. J. Mol. Biol. *157*, 105–132.

Loncar, D., and Singer, S.J. (1995). Cell membrane formation during the cellularization of the syncytial blastoderm of. Drosophila. Proc. Natl. Acad. Sci. USA *92*, 2199–2203.

Lupas, A., Van Dyke, M., and Stock, J. (1991). Predicting colied-coils from protein sequences. Science *252*, 1162–1164.

Masai, H., Miyake, T., and Arai, K. (1995). *hsk1*$^+$, a *Schizosaccharomyces pombe* gene related to *Saccharomyces cerevisiae* CDC7, is required for chromosomal replication. EMBO J. *14*, 3094–3104.

Maundrell, K. (1993). Thiamine-repressible expression vectors pREP and pRIP for fission yeast. Gene *123*, 127–130.

McCormick, S. (1993). Male gametophyte development. Plant Cell *5*, 1265–1275.

McNew, J.A., Parlati, F., Fukuda, R., Johnston, R.J., Paz, K., Paumet, F., Sollner, T.H., and Rothman, J.E. (2000). Compartmental specificity of cellular membrane fusion encoded in SNARE proteins. Nature *407*, 153–159.

Moreno, S., Klar, A., and Nurse, P. (1990). Molecular genetic analysis of fission yeast *Schizosaccharomyces pombe*. Methods Enzymol. *194*, 793–823.

Nakamura, T., Kishida, M., and Shimoda, C. (2000). The *Schizosaccharomyces pombe spo6*$^+$ gene encoding a nuclear protein with sequence similarity to budding yeast Dbf4 is required for meiotic second division and sporulation. Genes Cells *5*, 463–479.

Nakase, Y., Nakamura, T., Hirata, A., Routt, S.M., Skinner, H.B., Bankaitis, V.A., and Shimoda, C. (2001). The *Schizosaccharomyces pombe spo20*$^+$ gene encoding a homologue of *Saccharomyces cerevisiae* Sec14 plays an important role in forespore membrane formation. Mol. Biol. Cell *12,* 901–917.

Neiman, A.M. (1998). Prospore membrane formation defines a developmentally regulated branch of the secretory pathway in yeast. J. Cell Biol. *140*, 29–37.

Neiman, A.M., Katz, L., and Brennwald, P.J. (2000). Identification of domains required for developmentally regulated SNARE function in *Saccharomyces cerevisiae*. Genetics *155*, 1643–1655.

Novick, P., Ferro, S., and Schekman, R. (1981). Order of events in the yeast secretory pathway. Cell *25*, 461–469.

Pelham, H.R. (1999). SNAREs and the secretory pathway-lessons from yeast. Exp. Cell Res. *247*, 1–8.

Protopopov, V., Govindan, B., Novick, P., and Gerst, J.E. (1993). Homologs of the synaptobrevin/VAMP family of synaptic vesicle proteins function on the late secretory pathway in *S. cerevisiae*. Cell *74*, 855–861.

Rothman, J.E., and Orci, L. (1992). Molecular dissection of the secretory pathway. Nature *355*, 409–415.

Ruohonen, L., Toikkanen, J., Tieaho, V., Outola, M., Soderlund, H., and Keranen, S. (1997). Enhancement of protein secretion in *Saccharomyces cerevisiae* by overproduction of Sso protein, a late-acting component of the secretory machinery. Yeast *13*, 337–351.

Schulze, K.L., Broadie, K., Perin, M.S., and Bellen, H.J. (1995). Genetic and electrophysiological studies of *Drosophila* syntaxin-1A demonstrate its role in nonneuronal secretion and neurotransmission. Cell *80*, 311–320.

Sisson, J.C., Field, C., Ventura, R., Royou, A., and Sullivan, W. (2000). Lava Lamp, a novel peripheral Golgi protein, is required for *Drosophila melanogaster* cellularization. J. Cell Biol. *151*, 905–918.

Sollner, T., Whiteheart, S.W., Brunner, M., Erdjument-Bromage, H., Geromanos, S., Tempst, P., and Rothman, J.E. (1993). SNAP receptors implicated in vesicle targeting and fusion. Nature *362*, 318–324.

Tanaka, K., and Hirata, A. (1982). Ascospore development in the fission yeasts *Schizosaccharomyces pombe* and *S. japonicus.* J. Cell Sci. *56,* 263–279.

Tanaka, K., Yonekawa, T., Kawasaki, Y., Kai, M., Furuya, K., Iwasaki, M., Murakami, H., Yanagida, M., and Okayama, H. (2000). Fission yeast Eso1p is required for establishing sister chromatid cohesion during S phase. Mol. Cell. Biol. *20*, 3459–3469.

Thomas, P.S. (1980). Hybridization of denatured RNA and small DNA fragments transferred to nitrocellulose. Proc. Natl. Acad. Sci. USA *77*, 5201–5205.

Woods, A., Sherwin, T., Sasse, R., MacRae, T.H., Baines, A.J., and Gull, K. (1989). Definition of individual components within the cytoskeleton of *Trypanosoma brucei* by a library of monoclonal antibodies. J. Cell Sci. *93*, 491–500.

Yoo, B.Y., Calleja, G.B., and Johnson, B.F. (1973). Ultrastructural changes of the fission yeast (*Schizosaccharomyces pombe*) during ascospore formation. Arch. Mikrobiol. *91*, 1–10.

Zhang, R., Maksymowych, A.B., and Simpson, L.L. (1995). Cloning and sequence analysis of a cDNA encoding human syntaxin 1A, a polypeptide essential for exocytosis. Gene *159,* 293–294.